JOINT TRANSPORTATION
RESEARCH PROGRAM
INDIANA DEPARTMENT OF TRANSPORTATION
AND PURDUE UNIVERSITY

Improved Live Load Distribution Factors for Use in Load Rating of Older Slab and T-Beam Reinforced Concrete Bridges

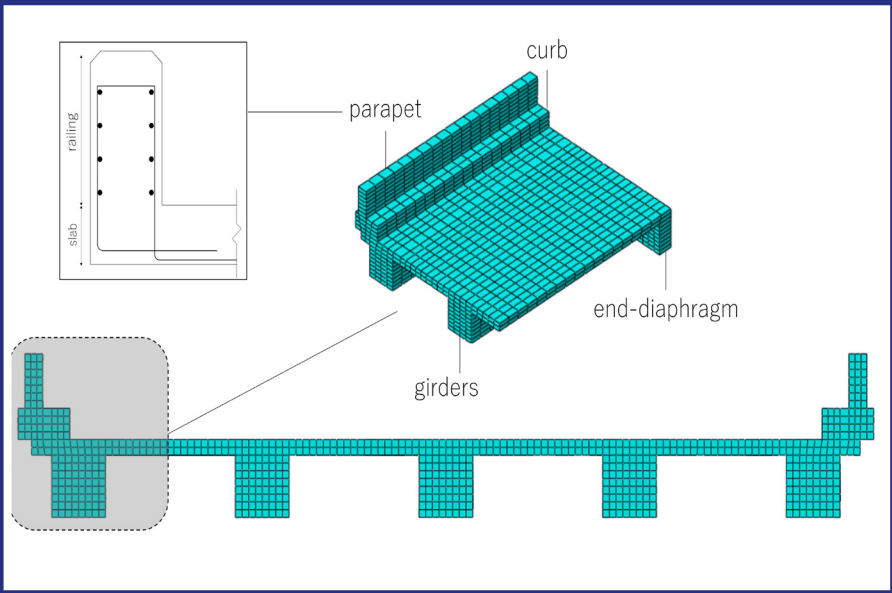

Faezeh Ravazdezh, Julio A. Ramirez, Ghadir Haikal

SPR-4444 • Report Number: FHWA/IN/JTRP-20121/06 • DOI: 10.5703/1288284317303

RECOMMENDED CITATION

Ravazdezh, F., Ramirez, J. A., & Haikal, G. (2021). *Improved live load distribution factors for use in load rating of older slab and T-beam reinforced concrete bridges* (Joint Transportation Research Program Publication No. FHWA/IN/JTRP-2021/06). West Lafayette, IN: Purdue University . https://doi.org/10.5703/1288284317303

AUTHORS

Faezeh Ravazdezh
Graduate Research Assistant
Lyles School of Civil Engineering

Julio A. Ramirez
Karl H. Kettelhut Professor and NHERI-NCO Center Director
Lyles School of Civil Engineering
Purdue University
(765) 494-2716
ramirez@purdue.edu
Corresponding Author

Ghadir Haikal
Senior Research Engineer
Southwest Research Institute

JOINT TRANSPORTATION RESEARCH PROGRAM

The Joint Transportation Research Program serves as a vehicle for INDOT collaboration with higher education institutions and industry in Indiana to facilitate innovation that results in continuous improvement in the planning, design, construction, operation, management and economic efficiency of the Indiana transportation infrastructure. https://engineering.purdue.edu/JTRP/index_html

Published reports of the Joint Transportation Research Program are available at http://docs.lib.purdue.edu/jtrp/.

NOTICE

TECHNICAL REPORT DOCUMENTATION PAGE

1. Report No. FHWA/IN/JTRP-2021/06	**2. Government Accession No.**	**3. Recipient's Catalog No.**
4. Title and Subtitle Improved Live Load Distribution Factors for Use in Load Rating of Older Slab and T-Beam Reinforced Concrete Bridges		**5. Report Date** January 2021 **6. Performing Organization Code**
7. Author(s) Faezeh Ravazdezh, Julio A. Ramirez, and Ghadir Haikal		**8. Performing Organization Report No.** FHWA/IN/JTRP-2021/06
9. Performing Organization Name and Address Joint Transportation Research Program Hall for Discovery and Learning Research (DLR), Suite 204 207 S. Martin Jischke Drive West Lafayette, IN 47907		**10. Work Unit No.** **11. Contract or Grant No.** SPR-4444
12. Sponsoring Agency Name and Address Indiana Department of Transportation (SPR) State Office Building 100 North Senate Avenue Indianapolis, IN 46204		**13. Type of Report and Period Covered** Final Report **14. Sponsoring Agency Code**

15. Supplementary Notes

Conducted in cooperation with the U.S. Department of Transportation, Federal Highway Administration.

16. Abstract

This report describes a methodology for demand estimate through the improvement of load distribution factors in reinforced concrete flat-slab and T-beam bridges. The proposed distribution factors are supported on three-dimensional (3D) Finite Element (FE) analysis tools. The Conventional Load Rating (CLR) method currently in use by INDOT relies on a two-dimensional (2D) analysis based on beam theory. This approach may overestimate bridge demand as the result of neglecting the presence of parapets and sidewalks present in these bridges. The 3D behavior of a bridge and its response could be better modeled through a 3D computational model by including the participation of all elements. This research aims to investigate the potential effect of railings, parapets, sidewalks, and end-diaphragms on demand evaluation for purposes of rating reinforced concrete flat-slab and T-beam bridges using 3D finite element analysis.

The project goal is to improve the current lateral load distribution factor by addressing the limitations resulting from the 2D analysis and ignoring the contribution of non-structural components. Through a parametric study of the slab and T-beam bridges in Indiana, the impact of selected parameters on demand estimates was estimated, and modifications to the current load distribution factors in AASHTO were proposed.

17. Key Words reinforced concrete bridge, live load distribution factor, finite element analysis, non-structural elements, modification factor	**18. Distribution Statement** No restrictions. This document is available through the National Technical Information Service, Springfield, VA 22161.

19. Security Classif. (of this report) Unclassified	**20. Security Classif. (of this page)** Unclassified	**21. No. of Pages** 45	**22. Price**

EXECUTIVE SUMMARY

Bridges are one of the most important components of transportation infrastructure systems, and they play a critical role within the highway and railway networks. According to the Federal Highway Administration (FHWA) of the U.S. Department of Transportation, there are more than 19,000 bridges located in the state of Indiana (FHWA, 2019). About 50% of the reinforced concrete bridges in service in Indiana were constructed before 1970, implying that they have exceeded their 50-year design life. Bridge construction in Indiana illustrates a significant uptick in reinforced concrete slab and slab-on-girder system designs in the decades of 1950 and 1960. These bridges represent an important component of the transportation network inventory still in function and are therefore required to satisfy current load-carrying capacity specifications known as the load rating procedure.

Demand assessment is one of the key aspects in the load rating of bridges. To assess demand, the bridge deck is subjected to standard vehicular live-loads and is typically analyzed using a simplified procedure based on a two-dimensional (2D) beam theory. In the Conventional Load Rating (CLR) method currently in use by the Indiana Department of Transportation (INDOT), T-beam bridges are analyzed using a girder-by-girder decomposition of the bridge, while flat-slab bridges are divided into 1-foot strips for the purpose of load rating. In this simple and rapid approach, the share of live loads for each beam is accounted for by using the Distribution Factor (DF). This factor reflects the effect of transverse live load distribution across the bridge width.

In *AASHTO Load and Resistance Factor Design Specifications* (AASHTO, 2014), distribution factors are related to geometrical features such as span length, deck width, slab thickness, and girder dimensions/spacing (for T-beam bridges). In LRFD provisions, skew correction factors are proposed to adjust the longitudinal moment and shear responses. However, the effect of secondary members has not been included in the development of current DF formulations. Edge-elements, such as curbs, railings, and end-diaphragms, impact bridge structural behavior by altering load distribution patterns across the bridge deck. Neglecting this effect could result in overestimated demand and, consequently, conservative rating factors for interior sections of the bridge superstructure.

Finite Element (FE) methods gained popularity in bridge studies to explore whole-system behavior compared to conventional member-by-member analysis. Three-dimensional (3D) models are capable of including bridge components that are neglected in current specifications and reflect their effects on bridge structural mechanisms. Therefore, their contribution in moment and shear responses can be simulated. The goal of this study was to investigate potential improvements in demand evaluation methodology for slab and T-beam bridges in Indiana using tools of FE analysis. A parametric study was conducted on samples of the two bridge types, focusing on the inclusion of secondary elements in the 3D models. Demand estimates obtained using FE analysis were compared with those of the AASHTO procedure. A statistical analysis of 3D demands on a select bridge sample was performed to estimate the effect of secondary elements on bridge shear and moment responses. To maintain the current procedure, new formulations for DFs were proposed that incorporate modification factors accounting for the effect of bridge features neglected in the development of distribution factor formulations.

Updated DFs can be used in conventional load rating methods to incorporate 3D effects while maintaining the simplicity of load rating procedures. Modification factors to current live load distribution factor formulations were identified to better represent the moment and shear responses observed from 3D finite element analysis and to address the limitations of the current procedure. The railing and diaphragm modification factors will be applied to the shear and bending moments from the 2D rating procedure using current distribution factors. The modifications are given for interior and exterior strips in slab bridges, and exterior and interior beams in T-beam bridges for cases of single and multi-lane loading configurations.

The findings of this study may be used to update the demand evaluation process used by the Indiana Department of Transportation for rating and design practices. The proposed modifications would benefit a great population of Indiana bridges that might be conservatively identified as structurally deficient or functionally obsolete. In particular, those bridges that show no signs of structural deficiency and, with proper maintenance, could be expected to serve well into the future.

CONTENTS

LIST OF TABLES

LIST OF FIGURES

1. INTRODUCTION

1.1 Motivation

Bridges are one of the most important components of transportation infrastructure systems and play a critical role within the highway and railway networks. According to the Federal Highway Administration (FHWA) of the U.S. Department of Transportation, there are more than 19,000 bridges located in the State of Indiana (FHWA, 2019). Figure 1.1 shows the construction year distribution of reinforced concrete bridge population in Indiana as of 2016. The figure shows that about 50% of the reinforced concrete bridges in service in Indiana were constructed before 1970, implying that they have exceeded their 50-year design life.

Bridge construction in Indiana illustrates a significant uptick in reinforced concrete slab and slab-on-girder system designs in the decades of 1950 and 1960. Based on the FHWA database, there are more than 3,000 slab and 700 T-beam bridges in Indiana. These bridges represent an important component of the existing network inventory still in function and are therefore required to satisfy current load-carrying capacity specifications known as the load rating procedure.

Demand assessment is one of the key aspects in the load rating of bridges. To assess demand, the bridge deck is subjected to standard vehicular live-loads and analyzed using a simplified procedure based on a two-dimensional (2D) beam theory. In the Conventional Load Rating (CLR) method currently in use by Indiana Department of Transportation (INDOT), T-beam bridges are analyzed using a girder-by-girder decomposition of the bridge, while flat-slab bridges are divided into 1-foot strips for the purpose of load rating. In this simple and rapid approach, the share of live loads for each beam is accounted for by using the Distribution Factor (DF). This factor reflects the effect of transverse live load distribution across the bridge width. Despite this methodology's favorability due to its simplicity, it has been reported that it could lead to an overestimation of members' live load share and consequent underestimation of the bridge rating factor. Results of field tests (Bell et al., 2013; Eom & Nowak, 2001) and analytical studies (Eamon & Nowak, 2004; Hasançebi & Dumlupinar, 2013; Jáuregui & Barr, 2004; Sanayie et al., 2016) conducted on existing bridges has indicated that such conservative evaluation could be attributed to ignoring three-dimensional (3D) behavior of bridge superstructure, simplifying the representation of members, and neglecting the effect of non-structural components such as curbs, barriers, sidewalks, and end-diaphragms. In particular, excluding secondary members in the structural analysis was found to be the main source of overestimation in the development of distribution factor formulation (Amer et al., 1999; Cai et al., 2007; Conner & Huo, 2006; Eamon & Nowak, 2002). Therefore, it is important to revisit the assumptions and principles of the method to identify potential areas of improvement for a more accurate assessment of bridge strength and load distribution.

Available computational tools facilitated full-scale bridge superstructure modeling to perform three-dimensional structural analysis. Finite Element (FE) methods gained popularity in bridge studies to explore whole-system behavior compared to conventional member-by-member analysis. 3D models are capable of including bridge components that are neglected in current specifications and reflect their effects on bridge structural mechanisms. Therefore, their contribution in moment and shear responses can be simulated. More importantly, with 3D models, the load distribution in the transverse direction of the deck can be explicitly represented.

1.2 Problem Statement

The Conventional Load Rating (CLR) method currently in use by Indiana Department of Transportation (INDOT) implies a distribution factor for demand calculations specified in American Association of State Highway and Transportation Officials (AASHTO). In *AASHTO Load and Resistance Factor Design Specifications* (AASHTO, 2014), distribution factors are related to geometrical features such as span length, deck width, slab thickness, and girder dimensions/spacing (for T-beam bridges). In LRFD provisions, skew correction factors are proposed to adjust the longitudinal moment and shear responses. However, the effect of secondary members has not been included in the development of current DF formulations. Edge-elements such as curbs, railings, and end-diaphragms

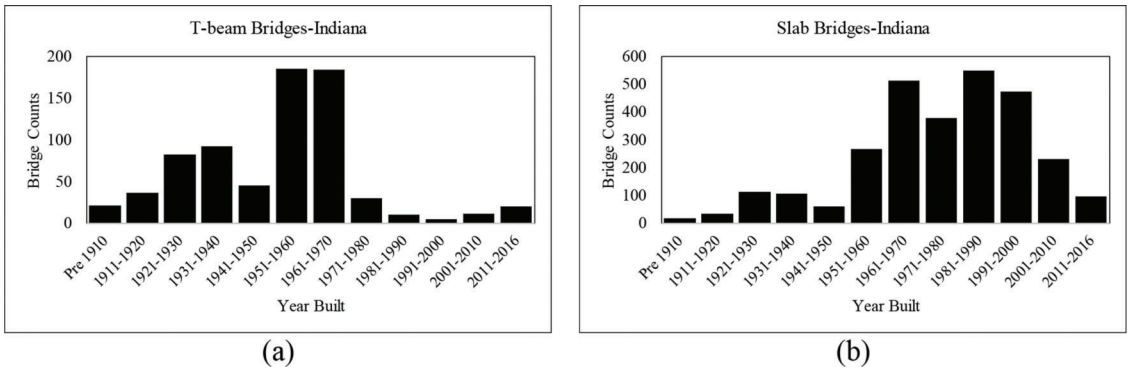

Figure 1.1 Bridge population in Indiana: (a) slab and (b) T-beam.

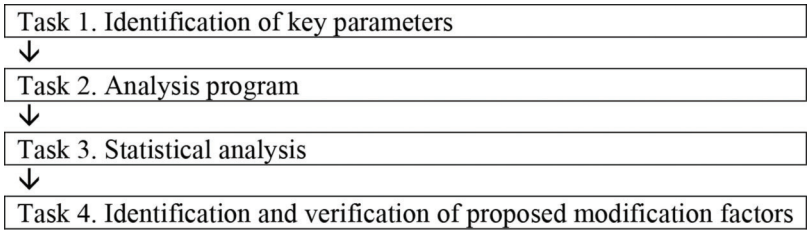

Figure 1.2 Research tasks of the project.

impact bridge structural behavior by altering load distribution patterns across the bridge deck. Neglecting this effect could result in overestimated demand and consequently, conservative rating factors for interior sections of the bridge superstructure. Improving demand estimates using 3D analysis can result in a more accurate assessment of bridge load-carrying capacity compared to CLR.

1.3 Research Objective and Plan

The goal of this study was to investigate potential improvements in demand evaluation methodology for slab and T-beam reinforced concrete bridges in Indiana using tools of FE analysis. A parametric study was conducted on samples of the two bridge types, focusing on the inclusion of secondary elements in the 3D models. Demand estimates obtained using FE analysis were compared with those of the AASHTO procedure. A statistical analysis of 3D demands on a select bridge sample was performed to estimate the effect of secondary elements on bridge shear and moment responses. To maintain the current procedure, new formulations for DFs were proposed that incorporate modification factors accounting for the effect of bridge features neglected in the development of distribution factor formulations. The tasks in this project, designed to achieve the project goal, are presented in Figure 1.2.

1.4 Report Overview

This report is presented in five chapters. Chapter 1 outlines the research motivation and problem statements followed by project objectives and plan. Chapter 2 includes a focused review of available literature on the live load distribution factor formulation. Moreover, the two types of Indiana bridges in the scope of this project were surveyed in the National Bridge Inventory (NBI) to identify key parameters used in the study. Chapter 3 explains the framework for the FE analysis program and 3D modeling of bridges used in the parametric study. A comparison of results obtained from conventional approaches and 3D finite element analysis are presented in this chapter. In Chapter 4 a statistical analysis on obtained FE results is conducted to propose modifications to current DF formulations. Potential improvements in the load distribution factor are discussed in this chapter. Lastly, Chapter 5 summarizes the key results of the study and provides recommendations for routine load estimate practices.

2. IDENTIFICATION OF THE KEY PARAMETERS

2.1 Literature Review

Live load Distribution Factor (DF) is designed to facilitate the computation of load distribution over the bridge deck in two-dimensional (2D) analysis. According to American Association of State Highway and Transportation Officials (AASHTO), this factor allocates the share of the live load in the transverse direction to each girder and beam strip in T-beam and slab bridges, respectively. This concept has been implemented in *AASHTO Load and Factor Design Specifications* (LFD) for T-beam bridges since the 1930s using empirical DFs, known to be in *S*/*D* format, where *S* is girder spacing and *D* the bridge type. These formulations were simple but accurate only within a specific range of geometrical parameters (Hays et al., 1986). It was argued that this form of formulation could lead to unrealistic results as some bridge characteristics influencing the distribution of loads were ignored (Bakht & Moses, 1988; Kuzmanovic & Sanchez, 1986). Moreover, the *S*/*D* equations, which form the basis of the distribution factor formulas, were only applicable to simply-supported non-skewed bridges and lost accuracy for continuous and/or skewed decks (Khaleel & Itani, 1990). Empirical DFs in standard specifications were used only with minor changes until 1994 when experimental tests and mathematical analyses were conducted on lateral live load distribution to investigate the accuracy of DFs (Bishara et al., 1993; Tarhini & Frederick, 1992; Zokaie et al., 1991).

Later, the DFs were revised based on a comprehensive study conducted on wheel loads distribution on highway bridges in the National Cooperative Highway Research Program, NCHRP 12-26 project, where the effect of different bridge features was investigated (Zokaie et al., 1991). Revised DF formulas provided higher accuracy than empirical equations by including additional bridge geometrical characteristics with a wider range of applicability (Mabsout et al., 1997a). These formulas were adopted by the AASHTO Load and Resistance Factor (LRFD) as the guide specifications for the distribution of live loads on highway bridges since 1994.

The NCHRP 12-26 project focused on the response of the bridge superstructures under a defined set of trucks specified by standard codes (HS trucks). The main objective of this project was to update provisions for DFs using refined analysis and propose simplified

methods for routine design and rating of bridges. The research was focused on more commonly used bridge types, including slab and slab-on-girder bridges. To study the range of applicability and common values of bridge parameters, a database of actual bridges was compiled, including 365 girder bridges (steel and prestressed/reinforced concrete). Span length/width, skew angle, number of girders, girder spacing, girder dimensions, slab thickness, and over-hang were considered variables in the parametric study performed in this project. A hypothetical average bridge was obtained with average properties. Using Finite Element (FE) analysis, parameters were varied one at a time in the average bridge model, and live load distribution factors were obtained for both shear and moment. Using statistical analysis, simplified formulas were developed to capture DF variation with each parameter for single and multiple-lane loadings. In the Zokaie et al. parametric study, it was assumed that the different parameters are independent of each other (1991). DFs were developed for simple-span non-skewed interior girders, and correction factors proposed to consider continuity, skewness, and girder-exteriority effects. The contribution of non-structural components, such as railings and diaphragms were neglected in this study.

Recent field tests and analytical studies have shown that the Zokaie et al. proposed modifications can be improved (Chen, 1999; Huo et al., 2004; Shahawy & Huang, 2001; Yousif & Hindi, 2007). It has been observed that neglecting the effect of diaphragms (Cai et al., 2002; Cai & Shahawy, 2004; Green et al., 2002), parapet/railings (Conner & Huo, 2006; Eamon & Nowak, 2002; Mabsout et al., 1997b), deck skewness (Barr et al., 2001; Khaloo & Mirzabozorg, 2003), and spans continuity (Mabsout et al., 1998) could result in conservative estimates of loads assigned to each girder when using the AASHTO LRFD distribution factor provisions.

In slab reinforced concrete bridges, the equivalent width strip (E), defined as the transverse distance over which a wheel line is distributed, plays the role of distribution factor to allocate a portion of the live load to each 1-ft. width beam strip. Like in girder bridges, it was claimed that empirical DF formulations for this type of bridge were not accurate before provisions of NCHRP 12-26 (Azizinamini et al., 1994a, 1994b). In the Zokaie et al. (1991) study, span length/width, skew angle, number of lanes, and slab thickness of 130 actual slab bridges were considered to obtain practical values of geometrical features of this bridge type. The DF formulation was developed following the same assumptions and procedure as in girder bridges. It must be noted that in the NCHRP 12-26 report, for the first time, bridge width and skew were geometrical parameters considered in the formulation of E. A limited number of studies were conducted to explore the accuracy and range of validity for flat-slab DFs. However, similarly to T-beam bridges, the effect of non-structural elements is not considered in the E provisions for slab reinforced concrete bridges. Neglecting the relatively high flexural stiffness of the barrier compared with the relatively low stiffness of the reinforced concrete slab impacts the demand estimation in exterior and interior beams or strips. Previous studies (Amer et al., 1999; Frederick & Tarhini, 2000; Mabsout et al., 2004; Menassa et al., 2007) have shown that ignoring this factor might overestimate the live load share of the equivalent interior beam strips and underestimate it on the exterior strips.

2.1.1 Gaps and Next Steps

In *AASHTO Load and Factor Design Specifications* (AASHTO, 2002), empirical distribution factors were only related to girder spacing in T-beam bridges and span length in slab bridges. In LFD provisions, the effect of skew and continuity of bridge spans on the distribution of loads was neglected. Based on the NCHRP 12-26 project findings, more geometrical features were included in the development of DF formulations such as bridge length, deck thickness, and girder dimensions in T-beam bridges and bridge width in slab ones. Skew correction factors were proposed to adjust the longitudinal moment and shear responses. DFs proposed in the 12-26 report were used in *AASHTO Load and Resistance Factor (LRFD) Specifications* with minor changes.

Table 2.1 and Table 2.2 summarize the evolution of DF formulations in the AASHTO specifications (LFD and LRFD). For slab bridges (Table 2.1), E, L, W, and N_l are equivalent strip width, individual span length, edge-to-edge bridge width, and number of lanes, respectively. In Table 2.2, for T-beam bridges, S, L, $K_g = n(I + Ae^2)$, and t_s are respectively girder spacing, span length, longitudinal stiffness, and slab thickness. d_e is horizontal distance from the centerline of the exterior web of exterior beam at deck level to the interior edge of curb or traffic barrier. In K_g formula, n is the

TABLE 2.1
Equivalent Strip Width (ft.) for Slab Bridges

	Flat-Slab Bridge	
	Moment and Shear Effect	
	Single-Lane Traffic	Multiple-Lane Traffic
AASHTO (LFD) 1970–2002	$4+0.06L \le 7$	
NCHRP (12-26) 1991	$0.5+0.25\sqrt{LW}$	$3.5+0.06\sqrt{LW}$
AASHTO (LRFD) 1994–present	$0.4+0.21\sqrt{LW}$	$3.5+0.06\sqrt{LW} \le \frac{W}{N_L}$

TABLE 2.2
Distribution Factors for T-Beam Bridges

	T-Beam Bridge								
	Moment Effect				Shear Effect				
	Interior Girder		Exterior Girder		Interior Girder		Exterior Girder		
	Single Lane Traffic	Multiple Lane (g_{Mm}) Traffic	Single Lane Traffic	Multiple Lane Traffic	Single Lane Traffic	Multiple Lane (g_{Vm}) Traffic	Single Lane Traffic	Multiple Lane Traffic
AASHTO (LFD)[a] 1970–2002	$\frac{S}{6.5}$ Lever rule if $S>6$	$\frac{S}{6}$ Lever rule if $S>10$	LR		–		–	
NCHRP (12-26) 1991	$0.1+\left(\frac{S}{4}\right)^{0.4}\left(\frac{S}{L}\right)^{0.3}\left(\frac{K_g}{12Lt_s^3}\right)^{0.1}$	$0.15+\left(\frac{S}{3}\right)^{0.6}\left(\frac{S}{L}\right)^{0.2}\left(\frac{K_g}{12Lt_s^3}\right)^{0.1}$	LR	$g_{Mm}\left(0.77+\frac{d_e}{9.1}\right)$	$0.6+\frac{S}{15}$	$0.4+\frac{S}{6}-\left(\frac{S}{25}\right)^2$	LR	$g_{Vm}\left(0.6+\frac{d_e}{10}\right)$
AASHTO (LRFD)[b] 1994–present	$0.06+\left(\frac{S}{14}\right)^{0.4}\left(\frac{S}{L}\right)^{0.3}\left(\frac{K_g}{12Lt_s^3}\right)^{0.1}$	$0.075+\left(\frac{S}{9.5}\right)^{0.6}\left(\frac{S}{L}\right)^{0.2}\left(\frac{K_g}{12Lt_s^3}\right)^{0.1}$	LR	$g_{Mm}\left(0.77+\frac{d_e}{9.1}\right)$	$0.36+\frac{S}{25}$	$0.2+\frac{S}{12}-\left(\frac{S}{35}\right)^2$	LR	$g_{Vm}\left(0.6+\frac{d_e}{10}\right)$

Note:
LR = Lever Rule.
[a]Distribution factor per wheel-line.
[b]Distribution factor per lane.

modular ratio between beam and slab materials, I is girder stiffness, A is girder area, and e is the eccentricity between centroids of girder and slab.

The effect of secondary members was not considered in the development of current DF formulations. In the present study, non-structural elements in three-dimensional (3D) modeling of bridge superstructure were explored, and their effect on the distribution of loads across the interior sections of the bridge deck was evaluated. Moreover, the demand estimated based on the 3D analysis in edge and interior parts was used to develop proposed modification factors for interior and exterior strips/girders. In both bridge types, skewed and continuous superstructures combined with secondary elements were modeled to investigate the possible interaction between these parameters and assess the reliability of available skew correction factors.

2.2 Statistical Distribution of Bridge Parameters

A total of 2,830 slab and 721 T-beam reinforced concrete bridges compiled in the National Bridge Inventory (NBI) database for the state of Indiana were surveyed to establish the typical bridge configurations to be considered in this project. Common ranges of geometrical characteristics such as number of spans, maximum span length, number of traffic lanes, curb-to-curb width, and deck skew angle were compiled using the data in the NBI. Figure 2.1 and Figure 2.2 illustrate relative frequency of mentioned variables for slab and T-beam bridges, respectively.

Among the bridges considered, single and three-span bridges dominated in both bridge types. Maximum span lengths for most bridges of the type considered in this study fell within the range between 20 ft. and 50 ft., with an average of 31 ft. and 34 ft. for slab and T-beam bridges, respectively. Roadway width for nearly half of the bridges in the database was within 20 ft. to 40 ft. This trend was consistent in flat slab and T-beam bridges. The average roadway widths were 33 ft. for the slab and 31 ft. for T-beam bridges. For both bridge types, two-lane bridges were predominant, accounting for about 80% of all the bridges. About 40% of the bridges were not skewed in both bridge types considered. Maximum skew angles of 65 degree and 55 degree were observed for slab and T-beam bridges, respectively.

Moreover, the research team reviewed bridge drawings for 35 slab and 210 T-beam Indiana bridges to identify possible geometrical features not shown in the NBI dataset, such as slab thickness, concrete compressive strength, girder numbers/dimensions/spacing for T-beam bridges, and railings and diaphragm dimensions. These values were used to represent cross-section dimensions of the reference model using average values. These reference models were used in the parametric study and statistical analysis discussed in Chapter 3 and Chapter 4 of this report. Figure 2.3 illustrates the geometrical features obtained from bridge drawings of slab and T-beam bridge cross-sections. Ranges of

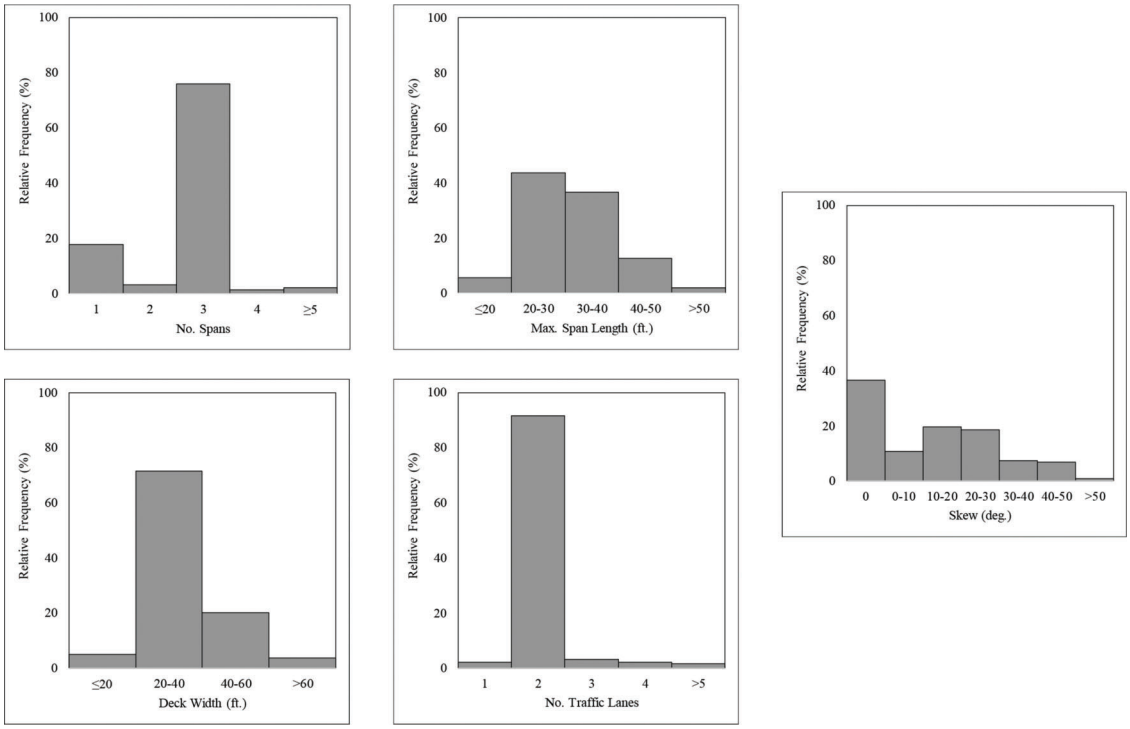

Figure 2.1 Distribution of geometrical parameters–slab bridges.

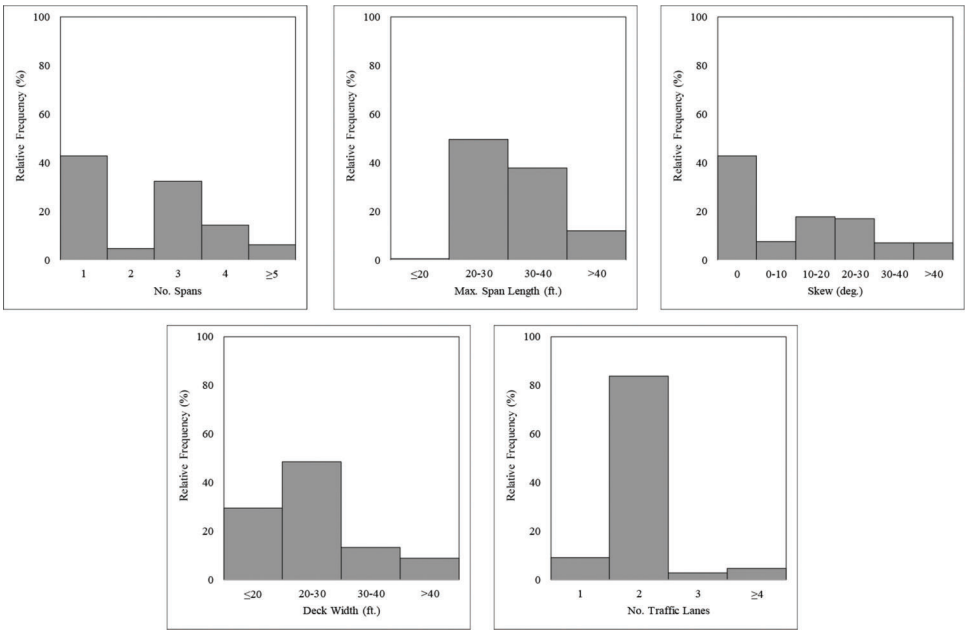

Figure 2.2 Distribution of geometrical parameters–T-beam bridges.

variation and average values of these parameters are summarized in Table 2.3.

2.3 Representative Sample Bridges

To determine the number of bridge samples for 3D modeling, parameters included in current DF formulations such as span length, deck width, slab thickness, and girder spacing/dimensions (for T-beams) were considered fixed variables. Parameters identified in the literature review as not included in previous work to develop DFs, such as railing height and width of end-diaphragms, were identified as variable parameters.

Despite the inclusion of skew and continuity factors in the DFs in current specifications, the number of spans and deck skew were considered variable parameters

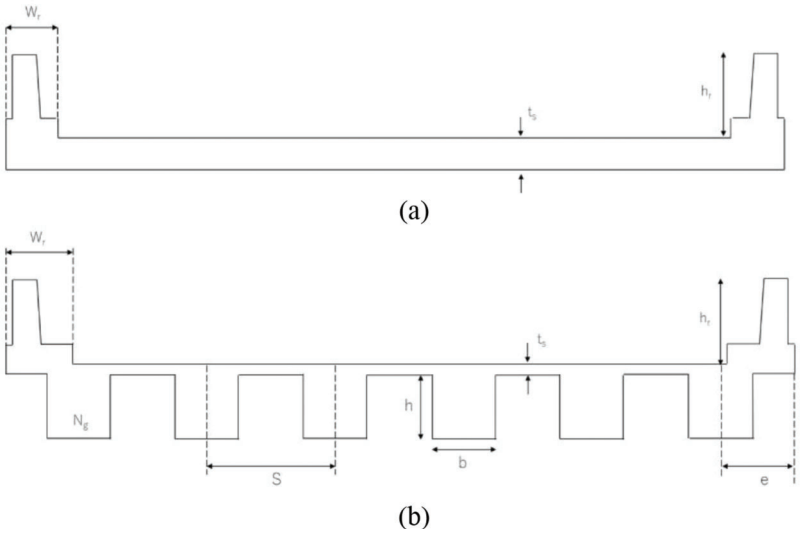

Figure 2.3 Geometrical parameters obtained from bridge drawings: (a) slab and (b) T-beam.

TABLE 2.3
Range of Cross-Sectional Parameters

Bridge Type	Variable	Range	Mean
Slab	Slab thickness (t_s)	8″–29″	17″
	Railing width (W_r)	1′–5.5′	1.5′
T-Beam	Slab thickness (t_s)	6″–10″	7″
	Number of girders (N_g)	4–9	5
	Girders spacing (S)	5′–9′	7′
	Beam height (h)	15″–63″	32″
	Beam width (b)	13″–32″	20″
	Eccentricity (e)	1′–3′	2′
	Railing width (W_r)	8″–80″	28″

TABLE 2.4
Parameters Values for Slab Bridge Models

Fixed Parameters	Deck width (W)	30′
	Slab thickness (t_s)	18″
	Span length (L)	29′
	Number of lanes (N_L)	2
	Railing width (W_r)	12″
Variable Parameters	Number of spans (N_s)	1–3
	Railing height (h_r)	0″ - 10″ - 20″ - 30″ - 40″ - 50″
	Skew angle (Θ)	0° - 10° - 20° - 30° - 40°

TABLE 2.5
Parameters Values for T-Beam Bridge Models

Fixed Parameters	Deck width (W)	32′
	Slab thickness (t_s)	7″
	Span length (L)	35′
	Number of lanes (N_L)	2
	Girders (N_g, b, h, S)	5 (20″ × 30″) at 7′
	Railing width (W_r)	10″
Variable Parameters	Number of spans (N_s)	1 - 3
	Railing height (h_r)	0″ - 15″ - 30″ - 45″
	Skew angle (Θ)	0° - 15° - 30° - 45°
	End-diaphragm width (W_d)	0″ - 5″ - 10″ - 15″

based on the conclusions of the SPR-4120 project (Seok et al., 2019). In this study, it was observed that these factors could change the effectiveness of secondary elements on lateral load distribution. Finally, although deck thickness in slab bridges is not included in the current DF formulation, in this study, it is considered as a fixed parameter since the findings of SPR-4120 suggested that there was no impact on the distribution of loads from changing the deck thickness.

Based on the statistical distribution of bridge parameters observed in the NBI dataset and review of bridge drawings by this research team, average values were obtained for fixed parameters, and a common range of variation was determined for variable ones. Fixed and variable parameters and their corresponding values are summarized in Table 2.4 and Table 2.5 for slab and T-beam bridge models, respectively. In total, 120 slab and 320 T-beam bridges were modeled in 3D to investigate the effect of variable parameters on load distribution and propose modifications to DFs.

3. ANALYSIS PROGRAM

With advances in modern computing resources, three-dimensional finite element analysis can be used to obtain reliable estimates of transverse load distribution in bridges, and systematically investigate possible improvements in bridge response estimates (Hasançebi & Dumlupinar, 2013; Sanayei et al., 2016). The main objective of the present study is to investigate longitudinal shear and moment demand across the bridge superstructure using 3D finite element analysis and

explore the possible refinement of live load distribution factors in T-beam and slab reinforced concrete bridges.

In the project SPR-4120, 3D finite element analysis was used effectively to model the bridge superstructure system when subjected to moving vehicles. 3D models were used to predict a more accurate lateral distribution of such live loads on bridge longitudinal girders/strips in a limited sample of representative reinforced concrete bridges (five T-beam and five solid slab of reinforced concrete). Using the tools of finite element analysis, the effect of simplifying assumptions used in conventional load rating on rating results was identified. This project expanded on sensitivity analysis to evaluate the effect of superstructure parameters, and it was noted that edge-elements significantly influenced the bending moment and shear force distribution across the bridge structure in studied bridges.

In Task 2 of the SPR-4444 project following the methodology of the NCHRP 12-26 project, bridge superstructures were modeled in 3D using Abaqus software and analyzed using the finite element method. Superstructure features, along with actual loading configurations, were explicitly represented in the model. In an extension to the NCHRP 12-26 project, in the SPR-4444, the contributions of parapets, railings and diaphragms were specifically considered. Critical values of moment and shear responses were obtained on different sections of the bridge superstructures. The obtained results were used to investigate the effectivity of studied parameters on bridge demand. A summary of assumptions, verification procedures, and results related to 3D modeling are presented in the subsequent sections.

3.1 Modeling Assumptions

A solid element type (C3D8R) was selected to model the bridge deck to investigate the 3D behavior of the superstructure. Solid elements allow full compatibility between the deck and integral edge components such as railings. The railings were modeled continuously with the slab part to ensure the edge participation in longitudinal stiffening. Particularly for T-beam bridge models with solid elements, full composite action could be imposed between slab and girders to prevent any slip and displacement between them.

A compressive strength ($f_c^{'}$) of 3,000 psi was assigned to concrete elements since this value was reported in bridge drawings for more than 87% of cases. Material properties were used assuming the behavior remains in the elastic range, and nonlinear behavior, including damage and plasticity, was not considered in this study. Supports were modeled assuming simple pin support at one end and roller one at the other end of the bridge span. For continuous bridges, middle supports were restrained using rollers. The supports were positioned on the bottom of the deck (slab bridges) and girders/diaphragms (T-beam bridges) to represent them sitting on columns/abutments.

3.1.1 Modeling Refinements

A convergence study was carried out with variable mesh sizes to find an element size that achieves a good balance between accuracy and computational time. The convergence study was performed on one arbitrary single-span slab bridge, comparing the maximum moment values for each refinement level. The slab bridge subjected to a HL-93 truck moving over the bridge span (50 ft.) close to the left curb. Figure 3.1 illustrates the moment responses using 2-in., 3-in., 6-in., and 10-in. mesh sizes. This figure shows that the results did not change significantly after 3-in. mesh, and therefore this element size was deemed suitable for the purpose of this study.

3.1.2 Model Partitioning

In flat slab bridges, the live load distribution factor provided in AASHTO is formulated for 1-ft. beam strips. Therefore, in the 3D modeling of slab bridge superstructures, the deck width was divided into 1-ft. beam strips and partitioned such that the moment and shear responses would be comparable with results obtained from the 2D analysis. As illustrated in Figure 3.2(a), 1-ft. strips comprised the interior sections of the bridge slab, while the railing component was included in exterior ones. This partitioning approach facilitated the calculation of demand estimate and DF separately for interior/exterior sections across the bridge deck. Figure 3.2(b) shows the interior and exterior girders partitioning method for T-beam bridges. In each girder, the flange width was equal to the girder spacing plus girder width. Like the slab case, the exterior girder in the T-beam model included the railing.

3.2 Live Load Application

Vehicular live loads were selected based on standard load configurations, as described in AASHTO LRFD. Truck HL-93 consists of three axle loads of 8, 32, and 32 kips spaced 14 ft. from each other, and the wheels

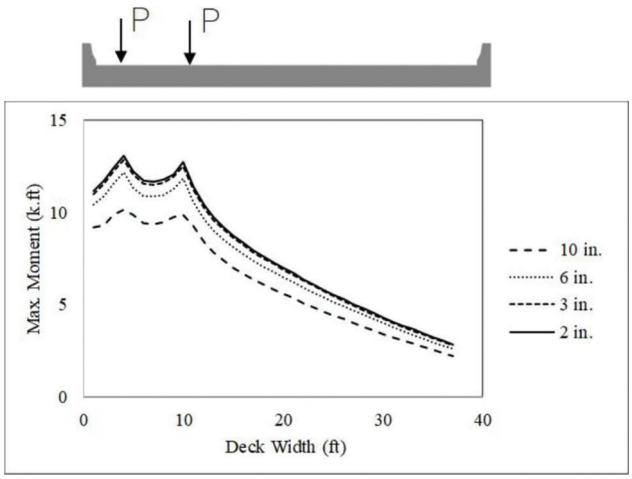

Figure 3.1 Convergence study.

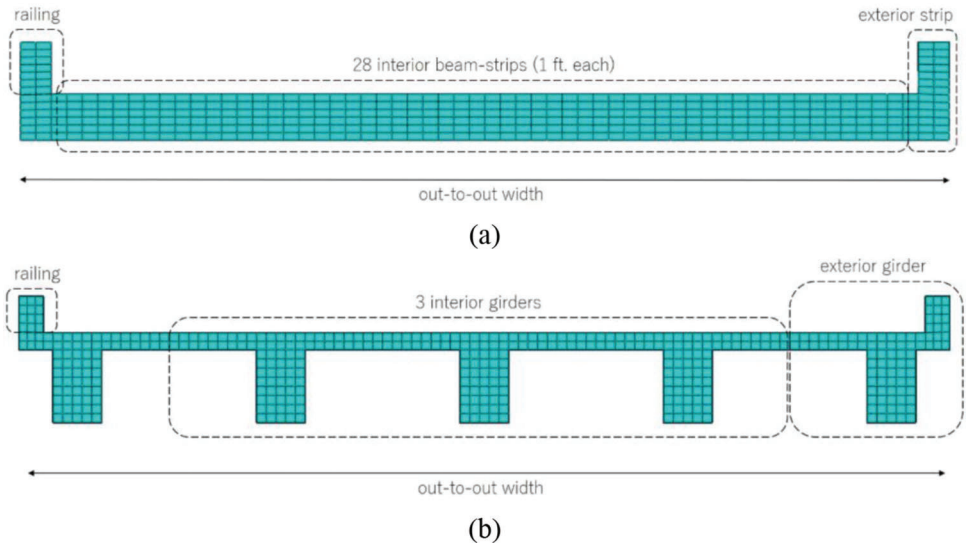

Figure 3.2 Partitioning approach for 3D bridge modeling: (a) slab and (b) T-beam.

are 6 ft. apart. AASHTO requires the spacing between the two 32 kips axles to be varied from 14 ft. to 30 ft. However, axle spacing was not varied in this study. For truck modeling, based on AASHTO recommendations, the wheel loads were applied using a rigid patch measured in 20-in. length and 10-in. width with equivalent pressure uniformly distributed over the contact surface instead of point loads to avoid stress concentration and convergence problems.

Trucks were moved step-by-step in the longitudinal direction (approximately every 6 in.) to produce maximum moment and shear responses and placed at multiple transverse positions across the bridge width to investigate the effect of lateral load distribution. The truck was positioned considering a 2-ft. distance between the first axle and the railing curb and a minimum of a 4-ft. distance between trucks for two-truck loading cases. Moreover, approach slabs were modeled on each end of the bridge span to accommodate trucks moving beyond the bridge deck, with the purpose of exploring the effect of partial loading on live load responses (refer to Figure 3.3).

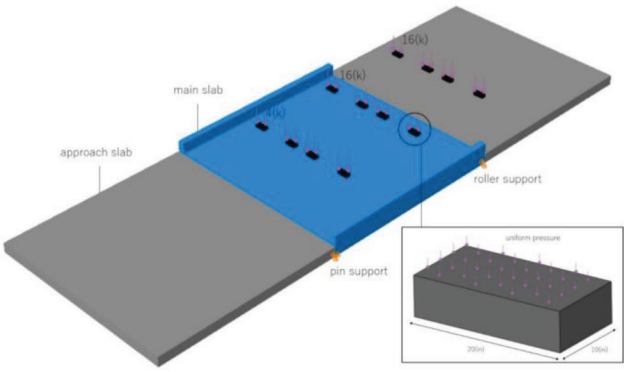

Figure 3.3 Truck load application in bridge 3D model analysis.

3.2.1 Truck Positioning

The HL-93 truck configuration was applied in single and multiple traffic-lanes over bridge width. In the case of multiple-lane loading, two trucks were positioned on the bridge superstructure since, according to the NBI database, more than 80% of bridges (slab and T-beam) accommodate two traffic lanes (see Figure 2.1 and Figure 2.2). To identify the critical loading position, trucks were moved along the span length on different transverse positions. In the case of slab bridges, trucks were moved every 2 ft. in transverse direction over the bridge width (Figure 3.4(a)), while for T-beam bridges, trucks were positioned over each girder, once placing one set of wheels on girder centerline and once placing the girder between two wheels (Figure 3.4(b)). This approach resulted in five loading configurations for single-lane and four loading configurations for multiple-lane loadings. It should be noted that loading configurations were applied to one half of superstructure width, taking advantage of symmetry.

One case of each bridge type was subjected to all loading configurations, and maximum values of moment and shear responses were obtained. These results were used to determine critical loading scenarios. According to results plotted in Figure 3.5, loading configurations 1-1 and 2-1 were most critical for exterior strip/girder. In these loading positions, trucks were located closest to the edge, resulting in higher stresses for the edge components. For slab bridges, the same loading configurations were critical for interior strips. However, in the case of T-beam bridges, loading positions of 1-2, 1-4, and 2-3 resulted in larger demand and, therefore, were selected as critical configurations for interior girders (girders 2 and 3). Narrowing down the loading cases to two and five critical ones optimized the analysis effort by decreasing the total number of 3D models to 120 for slab models and 320 for T-beam models instead of 540 and 576, respectively.

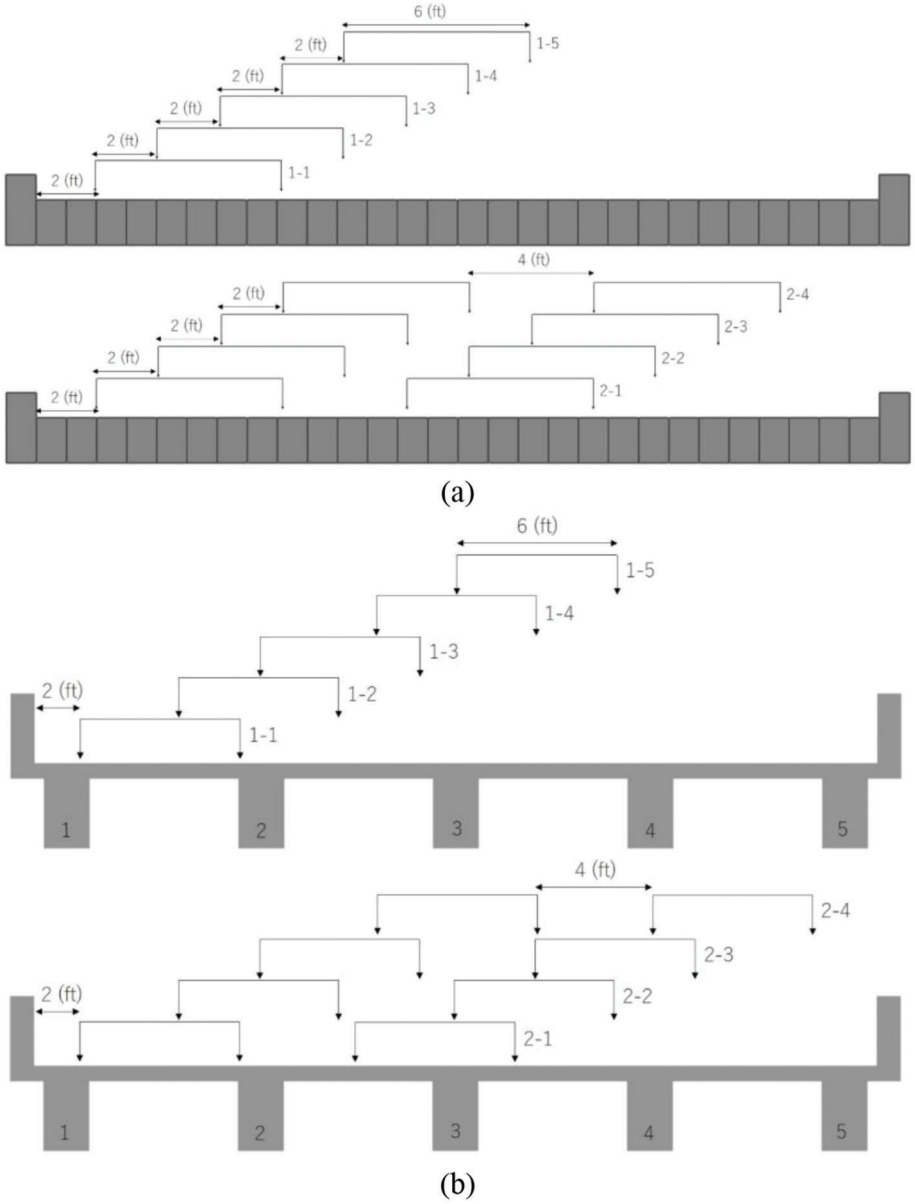

Figure 3.4 Truck loading configuration: (a) slab and (b) T-beam.

3.3 Model Validation

To investigate the reliability of the 3D modeling methodology adopted in this study, results obtained using FE analysis were compared to bridge test measurements (Cai et al., 2002). Strain measurements from a prestressed concrete bridge tested in Florida were compared with corresponding values obtained from 3D finite element analyses. This three-lane bridge is located on I-95 over Glades Road in St. Lucie County, Florida. It consists of six simply-supported spans. The tested span has a 125-ft. length and consists of nine AASHTO Type V prestressed concrete girders spaced at 6.5 ft. The deck is skewed at a 45 degree angle. Strain gages were installed on the bottom of the girders at 59 ft. from the left support. Two standard FDOT trucks rear axles were positioned at mid-span on the right and middle traffic lanes. Figure 3.6 shows the bridge dimensions and test/truck configurations.

Figure 3.7 illustrates a comparison of strain values obtained from the test and the 3D model. There is an acceptable agreement between the two sets of results. In the analysis of the 3D model, interior diaphragms, elastic bearings, among other field parameters, were not included in the analysis. Strain values obtained from FE analysis were matched pretty well to the results of a similar study conducted by Cai and Shahawy (plotted in Figure 3.7). They found that with detailed modeling

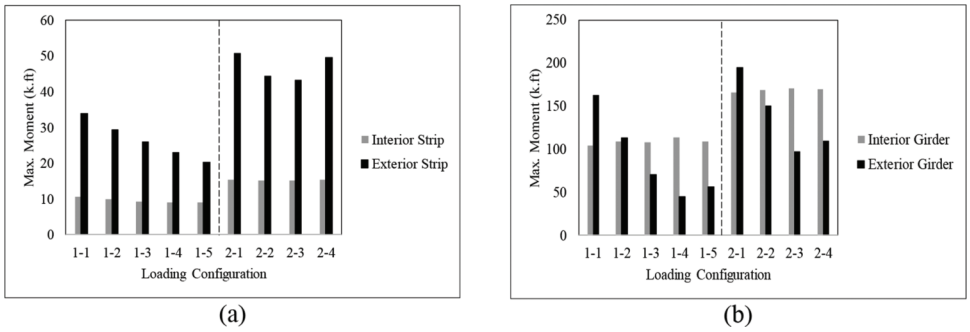

Figure 3.5 Maximum moment responses for different truck configurations: (a) slab and (b) T-beam.

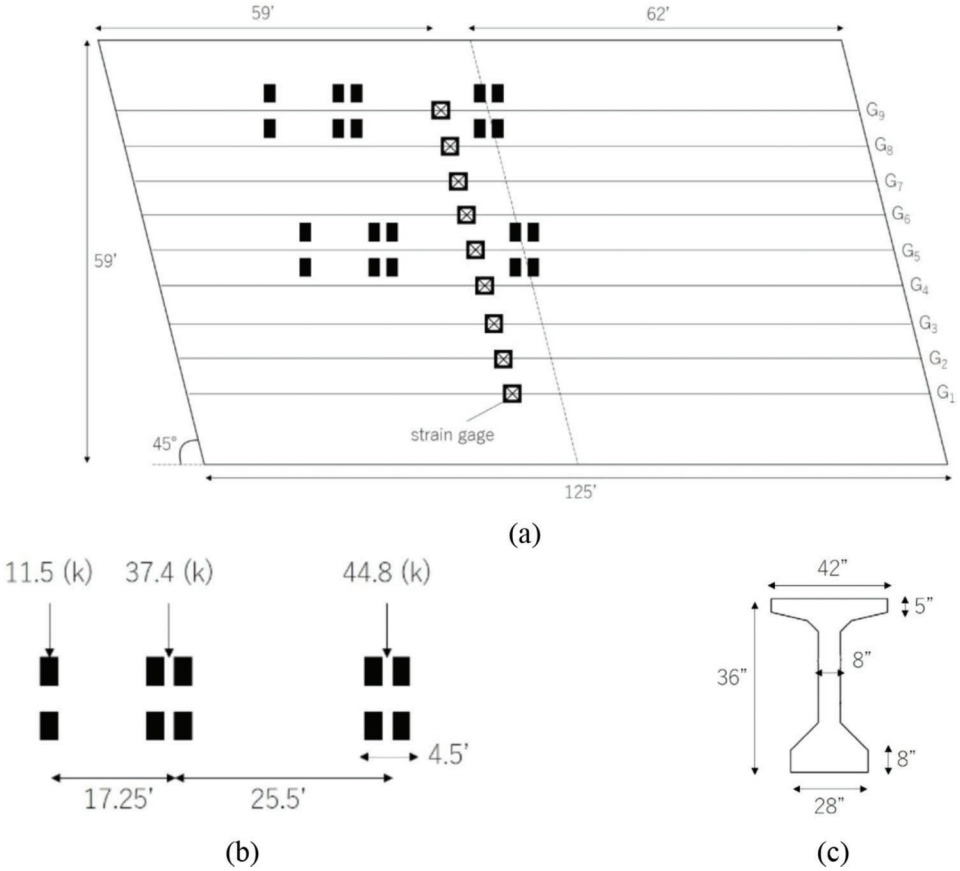

Figure 3.6 Test details: (a) bridge configuration, (b) truck load, and (c) girder dimensions.

of the intermediate diaphragms and elastic bearings, the discrepancy between the model and test results decreased. However, it was concluded that the original model could capture the pattern of strain distribution well and was sufficient for distribution factor estimates (Cai & Shahawy, 2004).

The calculated stresses in the solid elements were converted to moment and shear responses with a Python code. To verify the conversion process, the results were compared to corresponding envelopes obtained from 2D analysis. Figure 3.8 shows that the results are consistent for an arbitrary three-span bridge (85 ft.) subjected to one moving HL-93 truck. This bridge was modeled for validation purposes; secondary elements and deck skew angle were not considered in this model.

3.4 Reference Models

Two archetypical reference models, consisting of one solid slab and one T-beam, were defined to serve as benchmarks for comparison purposes. Reference models had decks with no skew and did not include secondary elements such as railings and end-diaphragms (in the case of T-beam models). For each bridge type (slab and T-beam), one reference model was a simple-span bridge, whereas the other one was considered

three-span to investigate the effect of continuity. In three-span models, equal length was considered for two exterior spans.The interior span length measured larger than the other two since this pattern was observed in bridge drawings. Average values of 1.25 and 1.4 were obtained for $\frac{L_{interior}}{L_{exterior}}$ in slab and T-beam bridges, respectively.

The slab reference model consisted of twenty-eight interior and two exterior strips while the T-beam model included three interior and two exterior girders. Dimensions of reference models were selected based on average values reported in Table 2.4 and Table 2.5. Figure 3.9 shows the cross-section dimensions of the reference bridge models.

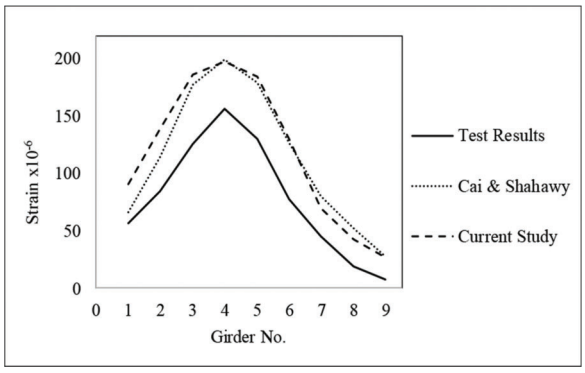

Figure 3.7 Test and FE strain results comparison.

3.5 Analysis Results

Values of the key parameters identified in Chapter 2 were varied in the reference models within the ranges observed in Section 2.2 (see Table 2.4 and Table 2.5 for slab and T-beam models, respectively). To study the effect of each variable, values of the key parameters were changed one at a time while other variables remained constant similar to the approach followed in the NCHRP 12-26 study. Then, to investigate the combined effect of variables on demand estimates, models were created with combination pairs of parameters. The range of values of the parametric study parameters is summarized in Table 3.1 and Table 3.2 for slab and T-beam models, respectively.

Sectional normal and shear stresses were obtained for interior and exterior strips/girders with various truck load configurations. Moment and shear envelopes along the strip/girder length were calculated using the Python code. An additional script was developed using Matlab to obtain peak moment and shear values for all

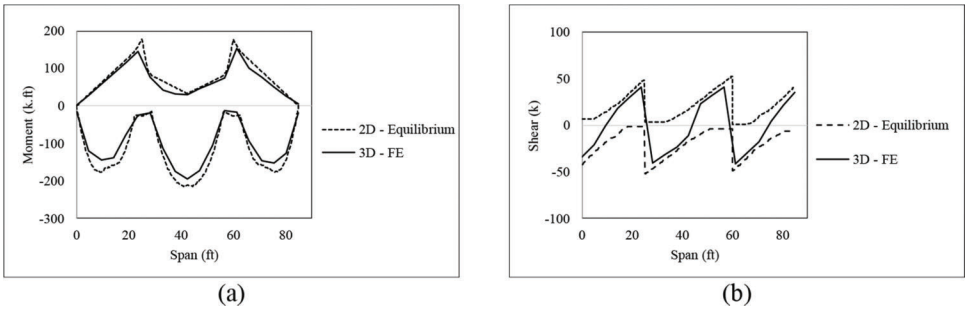

Figure 3.8 2D and 3D response comparison: (a) moment and (b) shear.

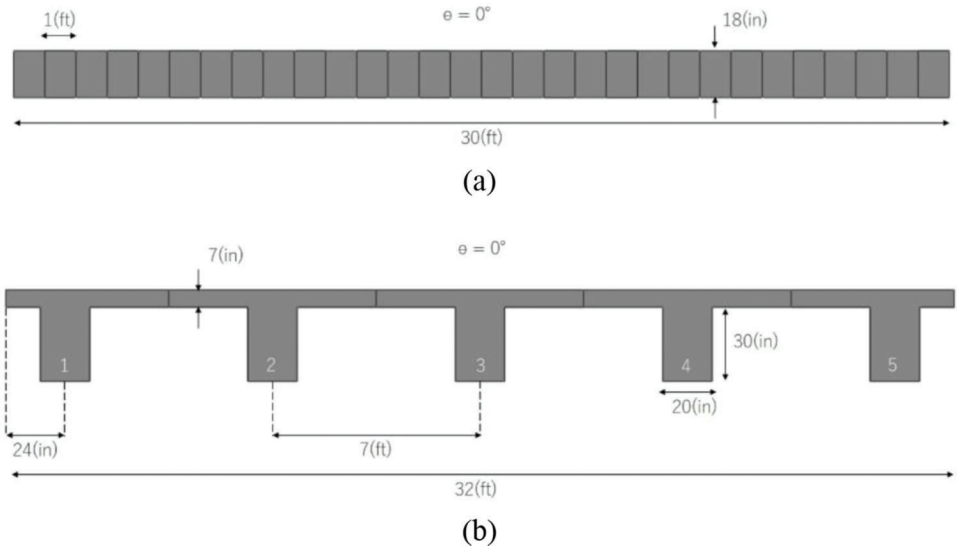

Figure 3.9 Reference models cross-section: (a) slab and (b) T-beam.

TABLE 3.1
Range of Parameter Values–Slab Models

Parameters and Range of Variation					
Skew (Θ) (deg.)	**0°**	**10°**	**20°**	**30°**	**40°**
Railing			0		
Height (h_r) (in.)			10		
			20		
			30		
			40		
			50		

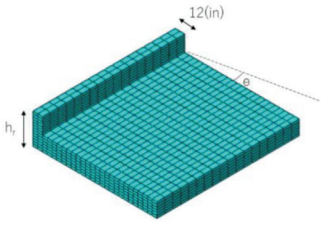

TABLE 3.2
Range of Parameter Values in the Analysis–T-Beam Models

Parameters and Range of Variation					
Skew (Θ) (deg.)	**0°**	**15°**	**30°**	**45°**	**Diaphragm Width (w_d) (in.)**
Railing Height (hr) (in.)		0			0
		15			
		30			
		45			
		0			5
		15			
		30			
		45			
		0			10
		15			
		30			
		45			
		0			15
		15			
		30			
		45			

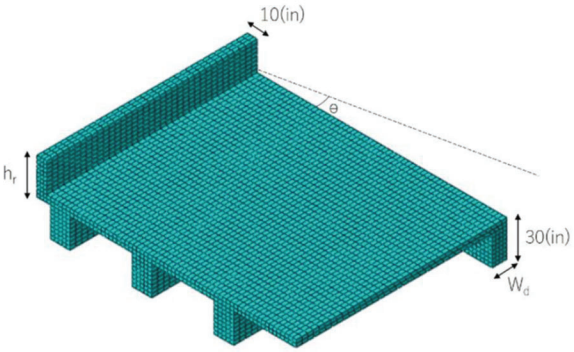

strips/girders. Using these results, the strip/girder with maximum demand values was identified as the critical one (see flowchart shown in Figure 3.10). Maximum values of shear and bending moment in the critical strip/girder (interior and exterior) were used to compare results for samples in the parametric study and calculate estimates of distribution factors.

The following analysis results are presented to evaluate the effect of the various variables on load distribution. It should be mentioned that the results of single-lane loadings are used in this discussion for the sake of brevity. However, results obtained for multiple-lane loadings will be presented in Chapter 4 and used in the statistical studies, along with those presented in this report. Herein only the individual effect of each variable is discussed. Results on the combined effect of variables are also part of Chapter 4.

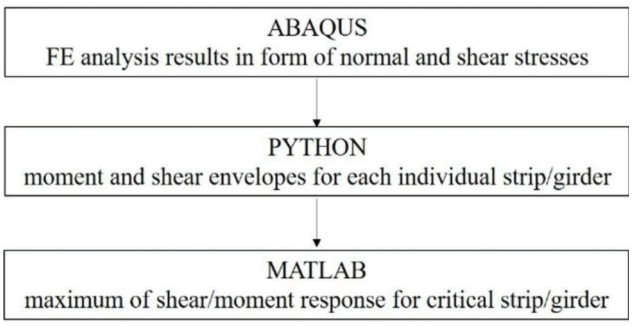

Figure 3.10 Procedure to obtain FEA results.

3.5.1 Railing Effect

To evaluate the effect of edge-stiffening elements on bridge demand, railings were added to the reference slab and T-beam models. Railings were modeled as fully coupled with the bridge deck using solid elements, allowing for full composite action between the two components. This assumption is valid for reinforced concrete railings and parapets properly anchored to the superstructure deck. Railing geometries were determined using representative cross-section dimensions of guardrails found in Indiana bridges. According to

standard drawings provided by INDOT, E706-BRSF and E706-BRPP railings are commonly used in slab and T-beam reinforced concrete bridges, respectively. A maximum design height of 45 in. in the BRSF and 42 in. in the BRPP is common. Since the variation in rail width is not as large as it is in heights, the width was considered constant, measuring 12 in. and 10 in. for slab and T-beam models, respectively (see sketches provided in Table 3.1 and Table 3.2). Therefore, six discrete values were considered for railing heights ranging from 0 in. to 50 in. for slab models, while in T-beam models, this variable was increased from 0 in. to 45 in. every 15 in. as specified in Table 3.1 and Table 3.2.

To examine the effect of variations in railing height, moment and shear demands were compared for models with and without (reference) railing. Figure 3.11 shows slab and T-beam models results as the railing height changes while other variables, skew angle and diaphragm width, were kept constant. Maximum shear and moment values of individual strips/girders are reported in Figure 3.12 when the HL-93 truck was located in position 1-1 (refer to Figure 3.4 for truck positions). This position illustrated the effect of railing height since the load was closest to the edge. The two peak moment/shear values observed at interior strips/girder correspond to the locations of the two truck axles (shaded red in graphs).

The presence of railings resulted in increased stiffness of the edge strip and girders compared to interior ones. The increased stiffness changed load distribution patterns across the bridge width by increasing the share of loading allocated to the exterior strip/girder. This also resulted in a decreased portion of load allocated to typical interior strips/girders. This effect can be observed in Figure 3.11, where the maximum responses of internal/external portions of the deck are shown across the bridge width. It is important to note that the increase in the share of the load in exterior strips of slab bridges was higher than in T-beam ones. This could be attributed to geometrical differences between the two edge cross-sections. In T-beam bridges, increases in railing height has a lower impact on the flexural stiffness of the combined railing-girder stiffness when compared to slab bridges. For slab bridges, the railing height (max. 50 in.) is relatively larger than slab thickness (18 in.), resulting in a larger stiffness difference between the exterior strip compared to interior ones.

Changes in moment and shear demands for different railing height values are shown in Figure 3.12, where the ratio represents a normalized demand value. This normalized value is calculated by dividing the demand obtained for different railing heights by the demand in the reference bridge without a railing. Thus, the demand ratio for the reference models is always 1, and the trend with increasing variable amounts can be more easily observed. In these graphs, the 2D demand ratio is represented as a constant value of 1 (dashed black line in Figure 3.12) since the edge-stiffening effect on interior sections' response is not considered in LRFD distribution factor formulations for slab and T-beam bridges.

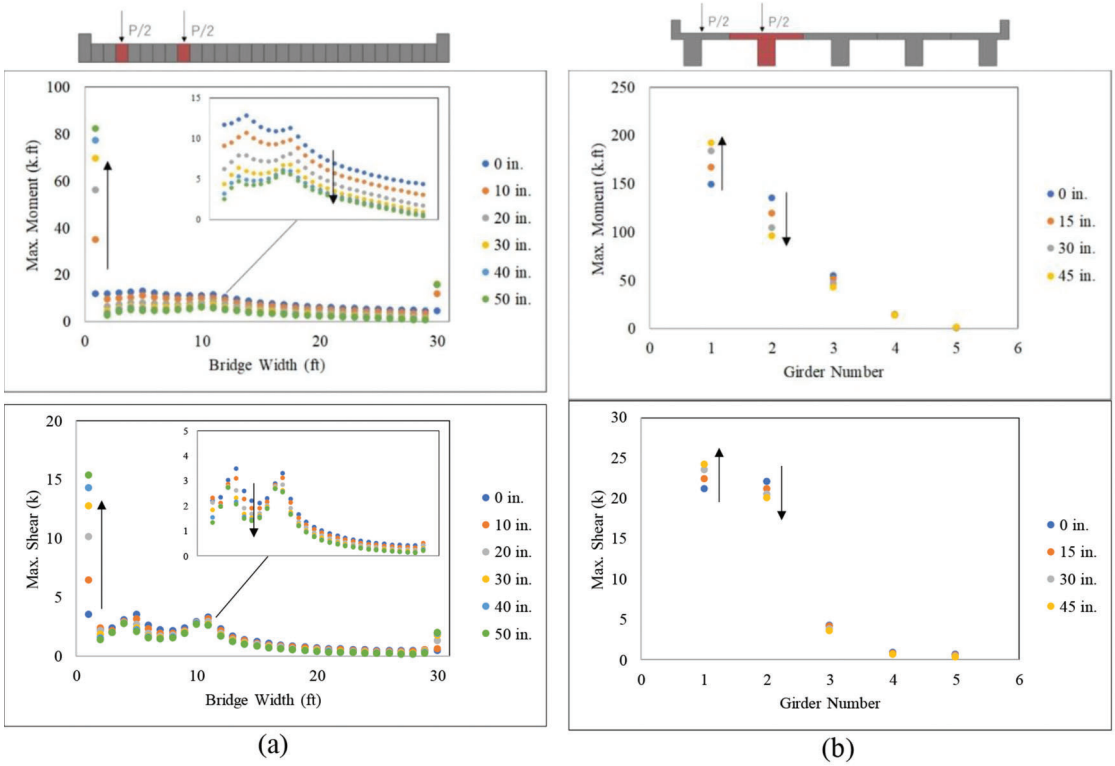

Figure 3.11 Railing effect on demand distribution across bridge width: (a) slab and (b) T-beam.

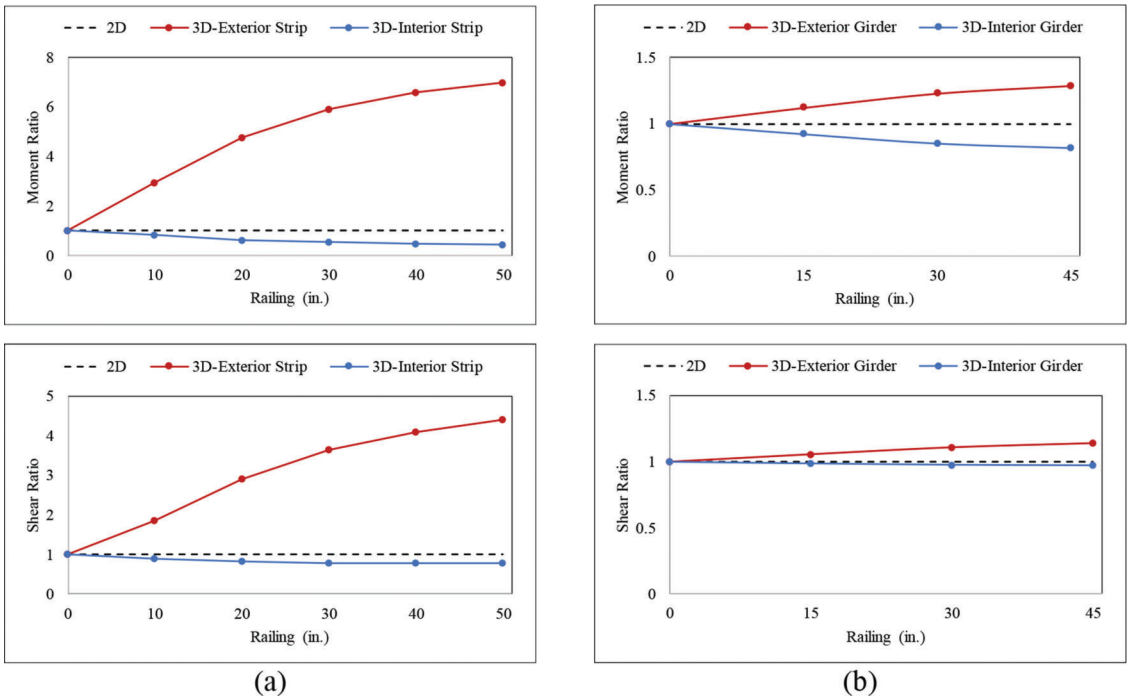

Figure 3.12 Railing height effect on maximum moment and shear: (a) slab and (b) T-beam.

In both bridge types, railing height increases resulted in a decrease in shear and moment in interior sections. However, this parameter had a higher impact on moments compared to shear values. In slab models, the increase in railing height led to a significant decrease in moments for interior strips while it increased in exterior strips. The reduction was almost 50% in the interior strips, while in exterior strips, it increased 6.8 times compared to the reference model. In terms of shears, exterior strips showed an increase of 4.3 times compared to the reference model, while the decrease in that of interior strips was about 22%. In the case of T-beam models, the larger increases were 28.8% in the moment and 13.9% in shear in exterior girders. In interior girders, maximum reductions of 18% in moments and 3% in shears were observed.

3.5.2 Skew Angle Effect

According to AASHTO, the skew angle is defined to be the angle between a normal/perpendicular to the alignment of the bridge and the centerline of the supports. Based on this definition, the reference model has a 0 degree skew angle. To evaluate the effect of this factor on the moments and shears in a slab bridge, the angles were increased from 0 to 40 degrees within 10-degree intervals. For T-beam models, four discrete values ranging from 0 to 45 degrees were considered for the skew parameter.

A comparison of FE results obtained from models with different skew angle values indicated that it changed the distribution of stress/strain across the bridge superstructure. Figure 3.13 shows the distribution and magnitude of normal and shear strains for two slab models, one with zero skew angle and the other with a 40 degree skew angle. These results correspond to the truck position associated with peak response. A reduction of almost 29% can be observed from Figure 3.13(a) for the maximum normal strain of the skewed bridge model compared to the one with zero skew angle. In the case of shear strain, peak magnitude was increased by a factor of 2.2 for the 40 degree skewed bridge. As illustrated in Figure 3.13(b), maximum shear occurred under load application for the non-skewed bridge, while shear strain concentration can be observed at the obtuse corner of the skewed deck. This resulted in an increase in shear forces at exterior strips. This pattern can be observed in Figure 3.14, where maximum responses are shown across the bridge deck for different skew values.

Results plotted in Figure 3.14 indicated a reduction in the longitudinal moment in interior and exterior strips/girders of slab and T-beam bridges with an increasing skew angle. In slab bridges, moment reduction up to about 30% was observed in interior and exterior strips for a deck skew of 45 degree. For interior/exterior girders, the maximum moment dropped by almost 40% when the skew angle of 45 degree was considered for T-beam models. Shear forces increased in exterior strips/girders when the skew angle was greater than 0 degrees. However, shear changes observed in interior ones were insignificant with respect to the skew angle (average of less than 3%).

In Figure 3.15, the maximum moment and shear demands for different skew values were normalized with respect to the response in the reference bridge ($\theta = 0^{\circ}$). In these graphs, ratios obtained from the finite element analysis were compared to corresponding skew correction factors specified in AASHTO (black dashed

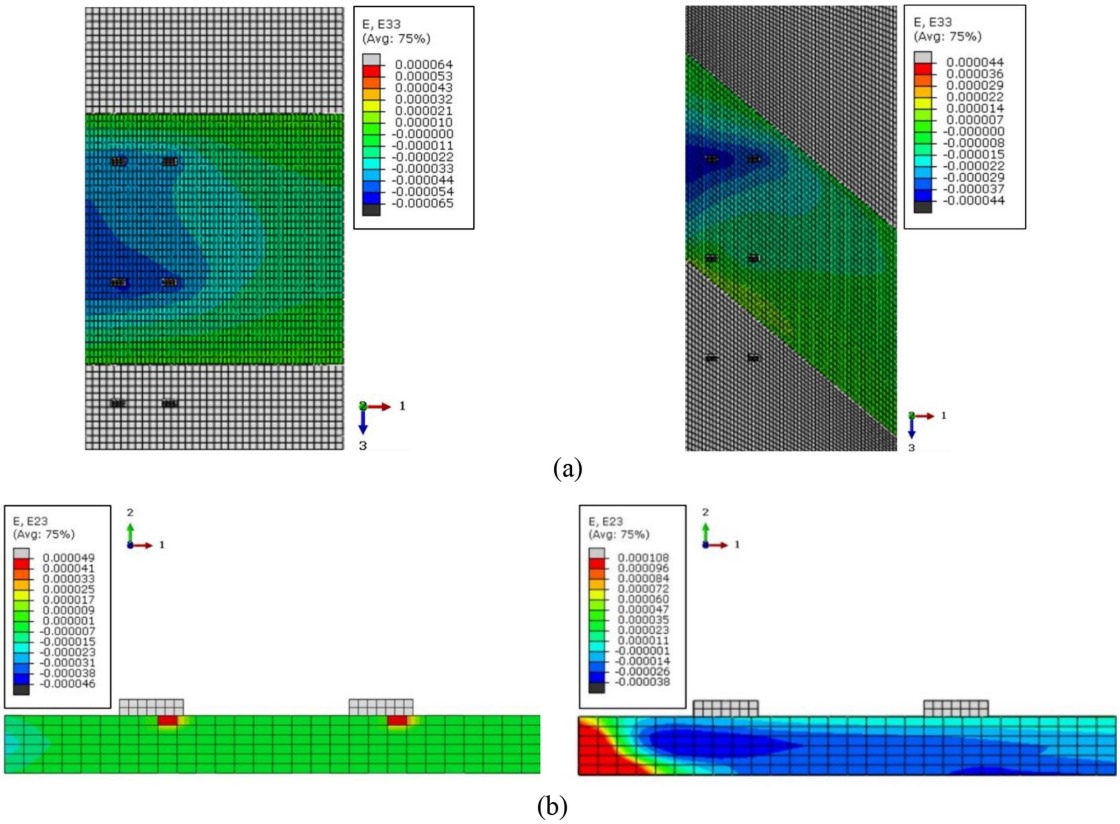

Figure 3.13 Strain distributions in skewed bridges: (a) normal strain and (b) shear strain.

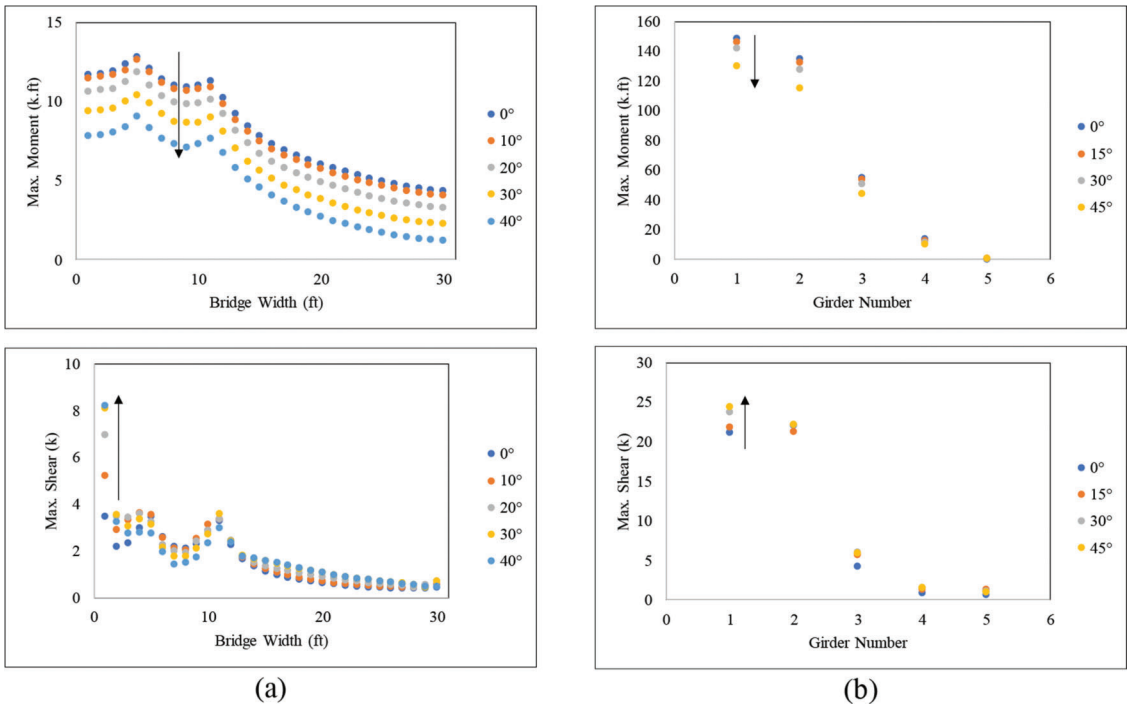

Figure 3.14 Skew angle effect on longitudinal moments and shears across the bridge: (a) slab and (b) T-beam.

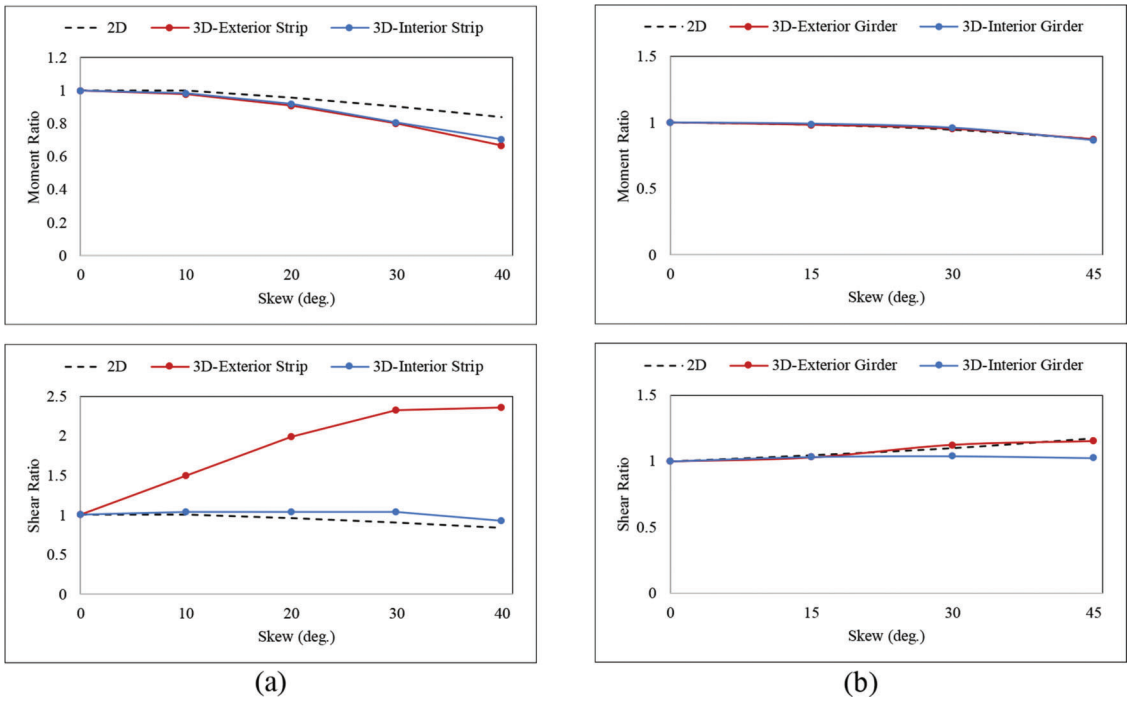

Figure 3.15 Skew effect on maximum longitudinal moment and shear: (a) slab and (b) T-beam.

line). In the AASHTO LRFD specifications, the correction factor is given in Article 4.6.2.3, Equation 4.6.2.3-3, to adjust moment/shear demand in skewed slab bridges. The skew correction factor formulation is shown in Equation 3.1, where θ stands for the skew angle. In T-beam bridges, the skew correction factor is specified in accordance with Tables 4.6.2.2.2e-1 and 4.6.2.2.3c-1 for moment and shear, respectively. The application of these factors reduces the bending moment (Equation 3.2) and increases the shear forces (Equation 3.3) for skewed T-beam bridges. In Equation 3.2 and Equation 3.3, S, L, $K_g = n(I + Ae^2)$, t_s, and θ are respectively girder spacing, span length, longitudinal stiffness, slab thickness, and skew angle. In K_g formula, n is the modular ratio between beam and slab materials, I is girder stiffness, A is girder area, and e is the eccentricity between centroids of girder and slab.

As shown in Figure 3.15(b), skew ratios obtained from 3D T-beam models were in good agreement with values obtained using the code-specified skew correction factor. For moment response, the average difference between 2D and 3D values was less than 1%. In terms of shear, this difference was about 5% and less than 1% for interior and exterior girders, respectively. Considering interior strips of slab models, 2D and 3D results varied with an average of about 7% for both moment and shear. However, the ascending pattern observed in Figure 3.15(a) indicated that the AASHTO skew factor formulation provided for interior strips of slab differs with 3D analysis results of shear forces in exterior strips. FE results suggested that a skew angle of 40 degree could result in an increase of 2.4 times the shear demand in exterior strips.

It should be noted that the observations on reduced longitudinal moment due to skew effect were consistent with the AASHTO correction factors specified for moment adjustment of skewed slab and T-beam bridges and therefore, modifications will not be proposed for this factor.

$$1.05 - 0.25\tan(\theta) \le 1 \qquad \text{(Eq. 3.1)}$$

$$1 - \left(0.25\left(\frac{k_g}{12Lt^3}\right)^{0.25}\left(\frac{S}{L}\right)^{0.5}\right)(tan\theta)^{1.5} \; 30^\circ \le \theta \le 60^\circ \qquad \text{(Eq. 3.2)}$$

$$1 + 0.2\left(\frac{12Lt^3}{k_g}\right)^{0.3} tan\theta \; 0^\circ \le \theta \le 60^\circ \qquad \text{(Eq. 3.3)}$$

3.5.3 End-Diaphragm Effect

The ends of reinforced concrete T-beam bridges typically have diaphragms. Four distinct diaphragm width values were implemented in the 3D models, while the diaphragm depth was kept constant and equal to girder depth (30 in.). A diaphragm width of 0 in. represents no diaphragm, i.e., the reference model. Figure 3.16 shows the demand variation as the diaphragm width was increased from 0 in. to 15 in. ($h_r = 0\,in., \theta = 0^\circ$).

Results shown in Figure 3.16 suggest that under any loading configuration, shear demand dropped by up to 15% for critical interior girders (those under applied load). However, increased shear was observed for the

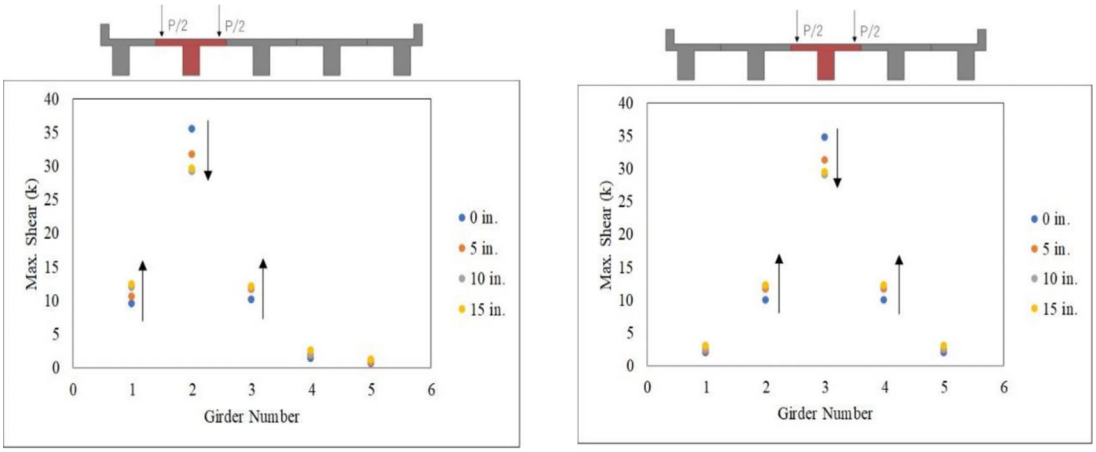

Figure 3.16 Diaphragm effect on demand distribution over bridge width.

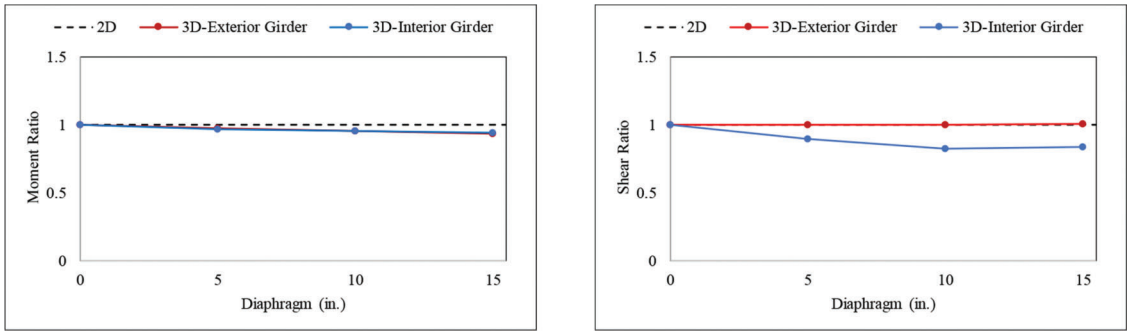

Figure 3.17 Diaphragm width effect on maximum longitudinal moment and shear.

adjacent girders (pointed out by arrows on graphs). This could be attributed to the presence of diaphragms enabling redistribution of forces by connecting the girders at the supports where maximum shear force occurs. In Figure 3.17, demand ratios of T-beam models with end-diaphragms were compared to the constant value of 1 for 2D diaphragm factor since this effect is not included in the demand estimate in LRFD specifications. The presence of diaphragms at span ends resulted in a negligible moment reduction (up to 6%) since stiffened edges are located far away from mid-span where maximum moment occurs. With a diaphragm width of 15 in., the shear force in interior girders was reduced by 16%. However, the shear results for exterior girders were relatively unchanged (less than 1% difference).

3.5.4 Continuity Effect

Slab and T-beam three-span bridges were modeled to examine the impact of continuity on the significance of the studied parameters. In slab bridges, the middle span was typically 29 ft., which corresponds to the span length of single-span bridges. The length of adjacent spans was taken as 23 ft. to enforce a ratio of spans length equal to 1.25 that matches the proportion observed in three-span bridges of the NBI dataset. For T-beam bridges, this value was 1.4, and therefore, span lengths were selected as 29-35-29 ft. Bridge cross-sections were modeled identical to that of the single-span bridge in both bridge types.

Similar to single-span cases, three-span reference models were non-skewed bridges without secondary elements. The key parameters were changed one at a time, and bridge responses were calculated under the loading discussed in Section 3.2.1. Figures 3.18, 3.19, 3.20, and 3.21 show the ratio of maximum shear and positive/negative moment to that in the reference model for each parameter considered. The parameters' range of variation is similar to that used in single-span models for each bridge type (see Table 3.1 and Table 3.2).

According to results presented in Figure 3.18, live-load responses decreased in interior strips/girders when railing was included in slab and T-beam three-span models. As expected, the opposite effect was observed in the exterior ones. It can be seen that the reduction in positive moment was slightly more than in the case of negative moment (about 2% on average for both bridge types). Similar to single-span bridges, shear demand was impacted less than moment. For slab bridges, increasing the railing height from 0 in. to 50 in. reduced shear, negative and positive moments by up to 12%, 40%, and 43%, respectively. Corresponding values (22% for shear and 55% for moment) obtained for single-slab models confirmed the observation that the effectiveness of edge-stiffening decreased for continuous bridges. In average, reduction in moment and shear

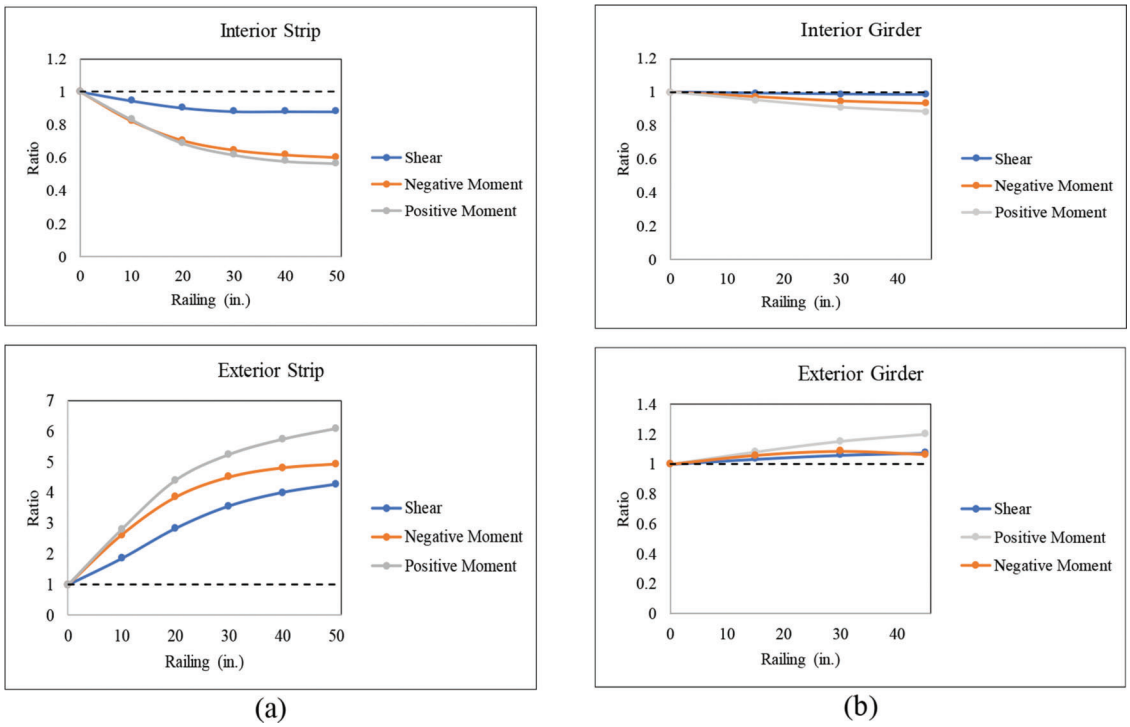

Figure 3.18 Effect of railing height in three-span bridges: (a) slab and (b) T-beam.

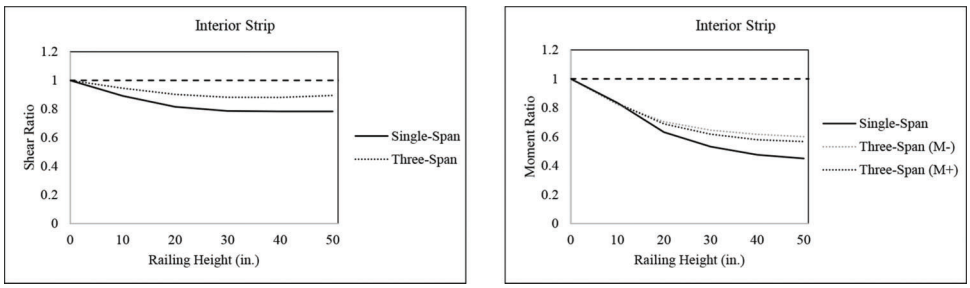

Figure 3.19 Rail effect in single-span vs. three-span slab bridge.

response of interior strips of three-span slab bridge was 0.8 and 0.5 times of those in a single-span bridge, respectively (see Figure 3.19). A similar pattern was observed in T-beam models with maximums of 1%, 7%, and 12% reduction in shear, negative moment, and positive moment, respectively. The corresponding values of shear and positive moment in the single-span T-beam models were 3% and 18%, respectively.

As illustrated in Figure 3.20, results in skewed three-span slab bridges showed that interior and exterior strips experienced up to 20% less bending moment on average. Shear forces for exterior strip increased by a factor of 2, while for interior strips, it decreased up to 7% for the skew angle of 40 degrees. These values were 12% (moment) and 7% (shear) in T-beam bridges.

In three-span T-beam bridges with end-diaphragms, moments and shears remained almost unchanged with respect to values in bridges with no diaphragm, less than 1% difference (Figure 3.21). The edge-stiffening effect of end-diaphragms decreased significantly due to the longer length of the bridge (almost tripled compared to the single-span bridge). Maximum shear and negative moment occurred at interior supports. This location was far enough from end-diaphragms to be influenced by their presence. Based on these results, the research team deemed that the effect on the negative moment and shear of the key parameters, i.e., railing height and end-diaphragms in three-span T-beam bridges was negligible when compared with those of the reference model. Therefore, this group was eliminated from the parametric study.

3.6 Summary of Findings

In the present chapter, a parametric study was conducted to assess the impact of geometrical parameters, including railing height, skew angle, and diaphragm width on moment and shear demand in slab and T-beam bridges. Railing height was confirmed as a parameter that produced the most drastic change in

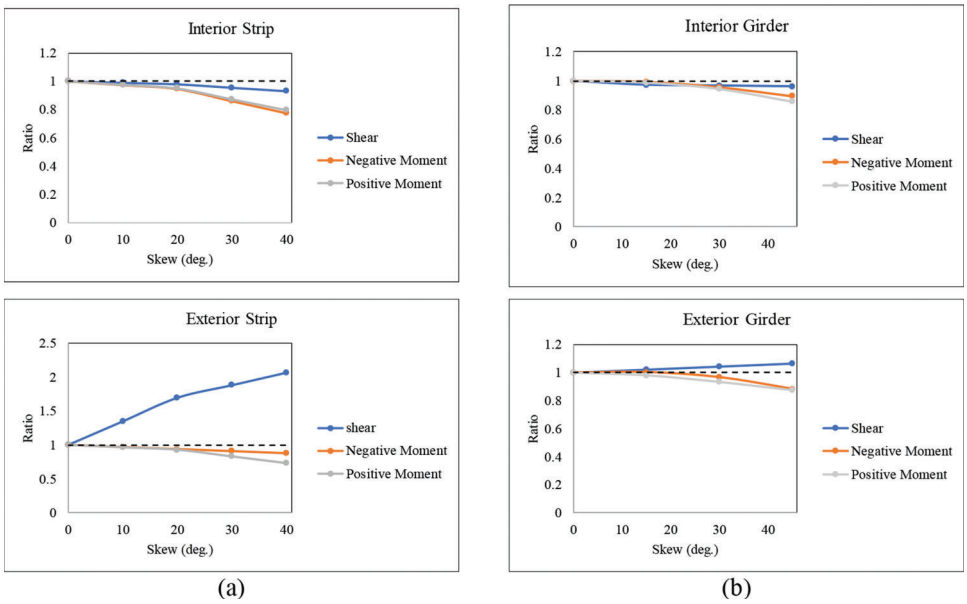

Figure 3.20 Skew effect in three-span bridges: (a) slab and (b) T-beam.

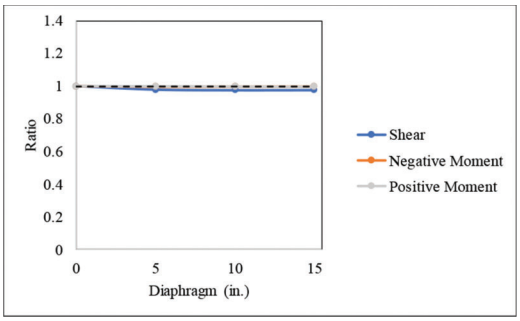

Figure 3.21 Diaphragm effect for three-span T-beam bridge.

moment and shear demands in bridges with respect to the reference models. When railing height was increased in slab models, moment and shear demands increased respectively by a factor of 7 and 4 in exterior strips. This resulted in a reduction of about 50% moment and 20% shear in interior ones. In the case of T-beam models, larger increases of about 29% in moment and 14% in shear were observed in exterior girders. In interior girders, maximum reductions of 18% in moments and 3% in shears were observed. The same pattern was observed for three-span bridges. However, it was observed that edge-stiffening efficacy decreased for continuous bridges.

Increases in the skew angle were found to result in a reduction in longitudinal moment in interior and exterior strips/girders for both single and three-span bridges. This observation was consistent with the AASHTO reduction factor specified for moment adjustment of skewed bridges. In exterior strips/girders, shear forces were increased for skew angles larger than 0 degree. In T-beam bridges, this observation was consistent with AASHTO recommendations for skew correction factor, and therefore, modifications will not be proposed for this factor. However, in slab bridges, the AASHTO skew factor provided for interior strips did not agree with 3D analysis results of shear forces in exterior strips.

The addition of diaphragms in single-span T-beam bridges at span ends resulted in reduced moment and shear responses in interior girders. However, this effect was negligible (about 1% difference) in three-span T-beam models. Since the effect of studied parameters on the negative moment and shear was negligible, this group was eliminated from the parametric study.

4. IDENTIFICATION AND VERIFICATION OF PROPOSED MODIFICATION FACTORS USING STATISTICAL ANALYSIS

Statistical methods include methodologies to collect, organize, and analyze a sample set of data. The goal of the statistical study is to utilize quantified models and representations to characterize a given set of data and draw conclusions that are appliable to the whole data population. For this purpose, the appropriate choice of the methods, sample selection, and statistical tests are of great importance. Herein, a parametric study was carried out on a sample of bridges to explore the effect of parameters such as railing height, skew angle, and diaphragm width on shear and moment demand estimates. The parametric study results used as a sample data set in a statistical study designed to obtain trends that apply to slab and T-beam bridge population in Indiana. In particular, demand ratios discussed in Section 3.5 were categorized as dependent variables, and studied parameters were categorized as independent ones. Statistical analysis was used to estimate the relationship between the variables and summarize the inferences into a mathematical form. This mathematical solution was formulated as modification factors that could be applied to current live load distribution factors

to incorporate the effect of secondary elements in bridge demand evaluations.

4.1 Data Collection

The first step in statistical analysis was the determination of variables. The main objective of this research was to investigate the effect of secondary elements on bridge response. 3D models were used to produce data (bridge responses) for the parameters considered in the study (bridge non-structural elements). As expressed in Equation 4.1, the demand ratio was defined as the maximum response of a bridge with variable parameters to the response of the reference model. Therefore, demand ratios of sample bridges obtained from FE analysis were considered as *dependent variables*. The height of railings, angle of skew, and the width of end-diaphragms were considered *independent variables*. The demand ratio for reference models, a constant value of 1, served as a benchmark to decide if a variable had a decreasing or increasing effect. Demand ratios could reach values greater or smaller than 1 depending on the effect of the independent variables. The ratios were calculated separately for shear/moment responses of interior/exterior strips or girders subjected to single/multiple-lane loading applications.

Based on this classification, dependent variables were represented as $Y(y_1...y_i)$ and independent variables were represented as $X(x_1...x_i)$ throughout this study. i ranges from 1 to n with n standing for sample size. According to variables and their corresponding values presented in Table 3.1 and Table 3.2, sample size was 30 and 64 for slab and T-beam sample bridges, respectively.

$$demand\ ratio = \frac{max.\ response\ in\ models}{reference\ model\ response} \qquad \text{(Eq. 4.1)}$$

4.2 Descriptive Statistics

All statistical definitions presented herein were adopted from *The Cambridge Dictionary of Statistics* (Everitt, 2002) and *A Dictionary of Statistics* (Upton & Cook, 2014), unless otherwise noted.

Descriptive statistics are generally used to describe the basic features of the data in a study. Mean, variance, and standard deviation are three main descriptive statistics describing the central tendency of a data set. Mean is arithmetic average, and variance is a measurement of the span of numbers in a dataset. Standard deviation, defined to be the square root of the variance, is used to indicate how far dataset values place from the mean. The mean and standard deviation were calculated to approximate the central tendency of variables in the sample data set. Moreover, these parameters were necessary for the calculation of other statistics used in statistical analysis. Mean and standard deviation, and range of variables are reported in Table 4.1 and Table 4.2 for slab and T-beam bridge models variables, respectively.

The correlation coefficient is a measure to estimate the statistical relationship between two sets of variables. This coefficient is defined as the covariance of the variables divided by the product of their standard deviations, as expressed in Equation 4.2. In Equation 4.2, r is the correlation coefficient, x, y and n are independent variable, dependent variable, and sample size, respectively. r ranges between ± 1. The magnitude of this coefficient indicates the relationship strength, and the sign shows the direction of the relationship. A coefficient value of 1 shows the strongest correlation, while a value of 0 indicates the lack of any linear relationship between the two variables.

The values of the correlation coefficient are summarized in Table 4.3. The positive correlation coefficients obtained for the variable of railing height in exterior sections indicated trend similarity between the variable and moment/shear responses in both bridge types. It confirmed that by increasing the railing height, responses in exterior sections of the bridge increases. The negative coefficients obtained for interior sections indicated the opposite trend. In general, the relationship was stronger in moment responses than for shear. Also, larger coefficients for demand in slab bridges compared to those in T-beams, indicated that the effect of the railing parameter was more significant in slab type bridges.

TABLE 4.1
Descriptive Statistics of Variables–Slab Bridges

Variables					Mean	Standard Deviation	Range
Independent Variables		Railing Height			25.00	17.37	0–50
		Skew Angle			20.00	14.38	0–4
Dependent Variables	Demand Ratio	Single-Lane	Moment	Interior Strip	0.60	0.18	0.4–1
				Exterior Strip	4.28	2.10	0.7–7.0
			Shear	Interior Strip	0.87	0.09	0.8–1.0
				Exterior Strip	3.44	1.07	1.0–4.8
		Multiple-Lane	Moment	Interior Strip	0.61	0.16	0.4–1.0
				Exterior Strip	3.96	1.97	0.6–6.8
			Shear	Interior Strip	0.89	0.09	0.7–1.0
				Exterior Strip	4.12	1.37	1.0–5.9

TABLE 4.2
Descriptive Statistics of Variables–T-Beam Bridges

Variables					Mean	Standard Deviation	Range
Independent Variable		Railing Height			22.50	5.63	0–45
		Skew Angle			22.50	16.90	0–45
		Diaphragm Width			7.50	16.90	0–15
Dependent Variable	Demand Ratio	Single-Lane	Moment	Interior Girder	0.82	0.09	0.7–1.0
				Exterior Girder	1.09	0.13	0.8–1.3
			Shear	Interior Girder	0.91	0.08	0.8–1.1
				Exterior Girder	1.10	0.05	1.0–1.2
		Multiple-Lane	Moment	Interior Girder	0.85	0.08	0.7–1.0
				Exterior Girder	1.11	0.14	0.8–1.4
			Shear	Interior Girder	0.88	0.12	0.6–1.0
				Exterior Girder	1.04	0.06	0.9–1.2

TABLE 4.3
Correlation Coefficients

	Loading Configuration		Single-Lane Loading				Multiple-Lane Loading			
	Demand Ratio		Shear		Moment		Shear		Moment	
Bridge Type	Section		Int.	Ext.	Int.	Ext.	Int.	Ext.	Int.	Ext.
Slab	Variable	Railing Height	-0.86	0.94	-0.90	0.95	-0.65	0.94	-0.72	0.91
		Skew Angle	0.02	0.18	-0.28	-0.21	-0.49	0.14	-0.58	-0.32
T-Beam		Railing Height	-0.01	0.51	-0.79	0.92	0.00	0.69	-0.27	0.87
		Skew Angle	-0.13	0.72	-0.49	-0.34	-0.94	-0.38	-0.92	-0.41
		Diaphragm Width	-0.73	-0.06	-0.27	-0.10	-0.19	0.08	-0.26	-0.07

Note:
Int. = interior strip/girder.
Ext. = exterior strip/girder.

Coefficient values obtained for the variable of diaphragm width in T-beam bridges showed no correlation between the variable and moment and shear responses in exterior girders. However, a negative correlation was observed for response in interior girders indicating that by increasing the width of the end-diaphragms, demand decreases in critical interior girders.

$$r(x,y)=\frac{n\sum xy-(\sum x)(\sum y)}{\sqrt{\left[n\sum x^2-(\sum x)^2\right]\left[n\sum x^2-(\sum x)^2\right]}} \quad \text{(Eq. 4.2)}$$

4.3 Regression Model

Regression is a statistical process to determine the numerical relationship between variables that are correlated (Weisberg, 2005). A regression model is presented as a mathematical formulation that relates the dependent variable (Y) to the independent variable (X). The former is referred to as the explained variable and the latter as the explanatory (regressor/predictor) variable. The regression analysis is performed on available data (observed pairs of (y_i,x_i)) to estimate the dependency function ($f(x_i)$) between the variables. The regression function $f(x_i)$ relates available data points (y_i,x_i) and, more importantly could be used for prediction purposes for data not included in the selected sample. The basic regression model is expressed in Equation 4.3 for $i = 1{:}\ n$ where n is the sample size. ε_i is an estimate of the individual errors.

$$y_i=f(x_i)+\varepsilon_i \quad \text{(Eq. 4.3)}$$

Classical regression theory considers the case of linear dependence; however, this assumption might be too restrictive for some problems (Spokoiny & Dickhaus, 2014). Equation 4.4 shows regression function in a multivariate linear form known as multilinear regression. Multilinear regression allows the inclusion of more than one independent variable in the model. Additional variables explain the part of Y that has not been explained by the existing variable. Consequently, they improve the prediction performance of the regression model. In Equation 4.4, a and b are regression coefficients known as intercept and slope, respectively. k is the number of predictors (X) included in the regression model. The sign of the slope indicates the direction of the relationship between the regressor and the dependent variable.

$$f(x)=a+b_1X_1+b_2X_2+\ldots+b_kX_k \quad \text{(Eq. 4.4)}$$

Linear regression functions can be extended to nonlinear ones using different forms of mathematical

functions instead of straight lines (Weisberg, 2005). More sophisticated functions such as polynomial, logarithmic, and power trendlines could improve the smoothness of the regression model and consequently increase the approximation accuracy. Moreover, a combination of predictors could be used in nonlinear regression models to reflect the joint effects of two or more variables. Products of predictors are called interactions. The use of interactions in a regression model with k predictors may expand/shrink the model to more/fewer than k terms.

In some problems with predictors within a different range of numbers, variables need to be scaled through a procedure known as the transformation of predictors (Washington et al., 2010). This process scales variables so that the regression model can capture the effect of all predictors in the same level to produce a reasonable approximation. Transformation (expressed in Equation 4.5) scales all variables within the range of 0 and 1. After finalizing the regression model, regression coefficients (intercept and slopes) should be transformed through a re-scaling process so that they apply to the original variables. In Equation 4.5, $\bar{x}_i$, x_i, *min*, and *max* represent scaled variable, original variable, minimum, and maximum values of variable set, respectively.

$$\bar{x}_i = \frac{x_i - min}{max - min} \qquad \text{(Eq. 4.5)}$$

4.4 Statistical Tests

There are different approaches to test the reliability of a statistical model, such as regression in statistics. The results of the tests indicate whether the model was sufficient to describe the studied data. Different numerical and graphical methods are used in the validation process which some examine the included variables while others investigate the performance of the statistical model. These include analysis of goodness of fit, regression residuals, and model validation. Statistical tests applied in the present study are summarized in the following subsequent sections.

4.4.1 Student T-Test

As explained previously, the first step in the regression procedure was to determine potential predictors. In multivariate regression models, where there is more than one variable to describe the outcome, it is critical to include crucial explanatories and disregard those that do not impact the results. The t-test is one of the statistical tools widely used to determine the significance of predictors included in a regression model. The t-test compares the statistical difference between two or more sets of data. If two sets of variables are statistically equal, then one set is not statistically significant and, therefore, should be eliminated from the list of regressors.

In the regression procedure, the t-statistic of each predictor should be compared to the t-value. The t-value is obtained using predefined t-tables shown in Figure 4.1. To use this table, the degree of freedom (*df*) and Confidence Level (CL) are needed. The degree of freedom is defined as $df = n - 1$ where n is the sample size. Confidence Level is a measure for the certainty of statistical results. CL of 95% is commonly used for statistical studies indicating that one can be 95% certain that the true value lies within the range denoted by the confidence interval (Winters et al., 2010). The confidence interval is usually assumed as twice the standard deviation. When the t-statistics for a given predictor is smaller than the t-value, that variable is identified as statistically insignificant and should not to be included in the regression model.

Moreover, application of the t-test on the regressors reduces the probability of having an over-parametrized regression function. This function might result in overfitting problem, which happens when a regression model is developed using too many numbers of parameters. Over-parametrized regression function might fit the sample data perfectly, but the performance decreases significantly when applied to another set of data. Moreover, the function seems more complicated and, therefore, not considered a user-friendly model.

4.4.2 Analysis of Residuals

In the regression procedure, the goal was to define a regression function that best fitted the data; however, assumption on the errors was inevitable. The residuals are estimates of the individual errors (ε_i) defined in Equation 4.3. Residuals are the differences between observed data (actual) and those predicted using the regression function. In statistics, the Residual Sum of Squares (RSS) is a measure of the efficiency of a regression model in explaining the data (Weisberg, 2005). This statistic estimates the amount of variance in a data set that is not captured by the model. Equation 4.6 expresses the formulation to calculate RSS where y_i and $f(x_i)$ are actual and predicted values, respectively. In an efficient regression model, RSS is minimized as much as possible.

$$RSS = \sum_{i=1}^{n} (y_i - f(x_i))^2 \qquad \text{(Eq. 4.6)}$$

4.4.3 Goodness of Fit

The goodness of fit of a statistical model describes the discrepancy between actual data and the predicted values obtained from a regression model. The coefficient of determination, also known as R-squared (R^2) is a measure of fitness that indicates how much the independent variable explains variation of a dependent variable. As expressed in Equation 4.7, R^2 ranges from 0 to 1. The coefficient of determination of 0 means the model cannot replicate the observed data, while the value of 1 for R^2 indicates that all predicted values perfectly matched with observed ones. When there are more than one regressors included in the model, the adjusted R-squared ($\bar{R}^2$) should be used to examine

the goodness of fit of the model in question (see Equation 4.8).

$$0 \le R^2 = 1 - \frac{LL(\beta)}{LL(0)} \le 1 \qquad \text{(Eq. 4.7)}$$

$$\bar{R}^2 = 1 - \frac{LL(\beta) - k}{LL(0)} \qquad \text{(Eq. 4.8)}$$

where $LL(\beta)$ and $LL(0)$ are log-likelihood at convergence and initial log-likelihood, respectively. k is the number of predictors. In this study, since there were more than one variable under investigation, the adjusted R-squared was used as an indicator of overall models fit.

4.5 Model Estimation Results

As discussed in Section 2.1, the effect of edge-elements was not included in the development of current distribution factor formulations. In this study, these parameters were included in 3D modeling of the bridges, and moment and shear responses were compared to a reference case without secondary elements. The difference was calculated as demand ratios in terms of moment and shear for interior and exterior sections of the superstructure. For each case, the value obtained for demand ratio was considered as a Modification Factor (MF) applicable to the live load distribution factor to incorporate the impact of parameters not included in the DF formulations as expressed in Equation 4.9.

In this study, Nlogit-4 software was used to conduct statistical analysis and estimate regression model parameters to formulize modification factors as a function of non-structural parameters (see Equation 4.9). Values of railing height (h_r), skew angle (θ), and diaphragm width (d_w) were inserted as independent variables in the multivariate regression model. Moreover, interactions (product of variables) were introduced to the model to capture the joint effect of the studied parameters. Different forms of mathematical functions (linear, polynomial, logarithmic, etc.) were defined for each variable to perform nonlinear regression analysis. Afterward, the student t-test method corresponding to a confidence interval of 95% was used to examine the significance of each variable in the model. To do so, t-ratios for each set of variables were calculated and then were compared to the t-value obtained from the standard t-table shown in Figure 4.1. The values of 2.045 and 2.000 were obtained for slab and T-beam datasets, respectively. Any set of variables with t-statistics less than reported t-values were considered statistically insignificant and therefore, disregarded from the regression procedure.

Since values of the dependent variable (MFs) and independent variables fell within different ranges, data transformation was applied using the scaling process explained in Section 4.3. In Nlogit-4, regression analysis was performed using the likelihood method. For each regression run, t-ratio, residual sum of square, and adjusted R-squared values were calculated as indicators of the performance of the model. Models with minimized RSS (closer to 0) and maximized $\bar{R}^2$ (closer to 1) were selected as finalized formulations to approximate the modification factors.

$$DF = DF_{code} * MF$$

Where,

$$MF = a + b_1 f(h_r) + b_2 f(\theta) + b_3 f(d_w) + b_4 f(h_r, \theta, d_w) \qquad \text{(Eq. 4.9)}$$

4.5.1 Proposed Modification Factors for Slab Bridges

In 3D models of slab bridges, the railing height was varied within the range of 0 in. to 50 in. based on feedback from the SAC members, and the skew angle was changed from 0 degree to 40 degree. Obtained modification factor formulations for slab bridges are a function of these two parameters however, correlation coefficients reported in Table 4.3 indicated that the railing parameter affected the results more significantly than the parameter of skew. Model estimation results are provided in Table 4.4 for transformed variables. Using the re-scaling procedure, regression coefficients were calculated for the original set of variables. Finalized modification factor formulations and the corresponding residual sum of square and adjusted R-squared values are summarized in Table 4.5. In the MF formulations, h_r is measured from the slab top surface in inches and the skew angle is measured in degrees. In non-skewed bridges with no railing on the edges, the value of 1 should be considered for MF in all cases.

MF results are plotted using regression models in Figure 4.2 and are compared to actual values obtained from the FE analysis for single-lane and multiple-lane loadings. A good agreement was observed between the results obtained from the two approaches. As shown in the graphs, MF formulations could capture the expected trend observed in actual data sets. Adjusted R-squared was 89.8% on average, indicating strong overall goodness of fit for the regression models.

As represented in Figure 4.2, MF values for interior strips were less than the value of 1, indicating a decreasing effect of the studied parameters on the moment and shear responses in internal sections. The factors are greater than 1 in the case of exterior strips showing that railing presence increased the demand in edge components of the superstructure. In general, the effects of railing and skew parameters were expressed by linear/quadratic and tangential trendlines in regression models, respectively. For all cases except shear in interior strips, the joint effect between railing and skew parameters was observed as expressed in the corresponding MF formulations by interaction variable of $h_r.tg\theta$ (refer to Table 4.5).

t Table

cum. prob	$t_{.50}$	$t_{.75}$	$t_{.80}$	$t_{.85}$	$t_{.90}$	$t_{.95}$	$t_{.975}$	$t_{.99}$	$t_{.995}$	$t_{.999}$	$t_{.9995}$
one-tail	0.50	0.25	0.20	0.15	0.10	0.05	0.025	0.01	0.005	0.001	0.0005
two-tails	1.00	0.50	0.40	0.30	0.20	0.10	0.05	0.02	0.01	0.002	0.001
df											
1	0.000	1.000	1.376	1.963	3.078	6.314	12.71	31.82	63.66	318.31	636.62
2	0.000	0.816	1.061	1.386	1.886	2.920	4.303	6.965	9.925	22.327	31.599
3	0.000	0.765	0.978	1.250	1.638	2.353	3.182	4.541	5.841	10.215	12.924
4	0.000	0.741	0.941	1.190	1.533	2.132	2.776	3.747	4.604	7.173	8.610
5	0.000	0.727	0.920	1.156	1.476	2.015	2.571	3.365	4.032	5.893	6.869
6	0.000	0.718	0.906	1.134	1.440	1.943	2.447	3.143	3.707	5.208	5.959
7	0.000	0.711	0.896	1.119	1.415	1.895	2.365	2.998	3.499	4.785	5.408
8	0.000	0.706	0.889	1.108	1.397	1.860	2.306	2.896	3.355	4.501	5.041
9	0.000	0.703	0.883	1.100	1.383	1.833	2.262	2.821	3.250	4.297	4.781
10	0.000	0.700	0.879	1.093	1.372	1.812	2.228	2.764	3.169	4.144	4.587
11	0.000	0.697	0.876	1.088	1.363	1.796	2.201	2.718	3.106	4.025	4.437
12	0.000	0.695	0.873	1.083	1.356	1.782	2.179	2.681	3.055	3.930	4.318
13	0.000	0.694	0.870	1.079	1.350	1.771	2.160	2.650	3.012	3.852	4.221
14	0.000	0.692	0.868	1.076	1.345	1.761	2.145	2.624	2.977	3.787	4.140
15	0.000	0.691	0.866	1.074	1.341	1.753	2.131	2.602	2.947	3.733	4.073
16	0.000	0.690	0.865	1.071	1.337	1.746	2.120	2.583	2.921	3.686	4.015
17	0.000	0.689	0.863	1.069	1.333	1.740	2.110	2.567	2.898	3.646	3.965
18	0.000	0.688	0.862	1.067	1.330	1.734	2.101	2.552	2.878	3.610	3.922
19	0.000	0.688	0.861	1.066	1.328	1.729	2.093	2.539	2.861	3.579	3.883
20	0.000	0.687	0.860	1.064	1.325	1.725	2.086	2.528	2.845	3.552	3.850
21	0.000	0.686	0.859	1.063	1.323	1.721	2.080	2.518	2.831	3.527	3.819
22	0.000	0.686	0.858	1.061	1.321	1.717	2.074	2.508	2.819	3.505	3.792
23	0.000	0.685	0.858	1.060	1.319	1.714	2.069	2.500	2.807	3.485	3.768
24	0.000	0.685	0.857	1.059	1.318	1.711	2.064	2.492	2.797	3.467	3.745
25	0.000	0.684	0.856	1.058	1.316	1.708	2.060	2.485	2.787	3.450	3.725
26	0.000	0.684	0.856	1.058	1.315	1.706	2.056	2.479	2.779	3.435	3.707
27	0.000	0.684	0.855	1.057	1.314	1.703	2.052	2.473	2.771	3.421	3.690
28	0.000	0.683	0.855	1.056	1.313	1.701	2.048	2.467	2.763	3.408	3.674
29	0.000	0.683	0.854	1.055	1.311	1.699	2.045	2.462	2.756	3.396	3.659
30	0.000	0.683	0.854	1.055	1.310	1.697	2.042	2.457	2.750	3.385	3.646
40	0.000	0.681	0.851	1.050	1.303	1.684	2.021	2.423	2.704	3.307	3.551
60	0.000	0.679	0.848	1.045	1.296	1.671	2.000	2.390	2.660	3.232	3.460
80	0.000	0.678	0.846	1.043	1.292	1.664	1.990	2.374	2.639	3.195	3.416
100	0.000	0.677	0.845	1.042	1.290	1.660	1.984	2.364	2.626	3.174	3.390
1000	0.000	0.675	0.842	1.037	1.282	1.646	1.962	2.330	2.581	3.098	3.300
z	0.000	0.674	0.842	1.036	1.282	1.645	1.960	2.326	2.576	3.090	3.291
	0%	50%	60%	70%	80%	90%	95%	98%	99%	99.8%	99.9%
	Confidence Level										

Figure 4.1 Student t-test distribution (Everitt, 2002).

It should be noted that in slab bridges, studied parameters affected moment demand more compared to shear demand resulting in larger regression coefficients in moment MF formulations. Moreover, higher residuals were observed in shear regression models since shear FE results had fewer specific trends than moment ones.

4.5.2 Proposed Modification Factors for T-Beam Bridges

In 3D models of T-beam bridges, the railing height was varied within the range of 0 in. to 45 in., the end-diaphragm width within 0 in. to 15 in., and the skew angle from 0 degree to 40 degree. Therefore, the proposed modification factor formulations for T-beam bridges contain a combination of these three parameters. Table 4.6 provides model estimation results for transformed variables used in the re-scaling procedure to obtain regression coefficients for the original set of variables. Finalized modification factor formulations are summarized in Table 4.7 along with the corresponding residual sum of square and adjusted R-squared values. In the MF formulations, h_r and d_w are measured in inches and skew angle is measured in degrees. Similar to slab bridges, in non-skewed T-beam bridges without edge-elements, the value of 1 should be considered for MF in all cases.

MF regression results are compared with actual values obtained from the 3D FE analysis for single-lane and multiple-lane loading applications in Figure 4.3. A good agreement was observed between the results obtained using the two procedures with R-squared values ranging from 0.72 to 0.98. MF formulations were able to capture expected increasing/decreasing trends that were observed in actual data. As shown in the graphs, MF values for interior girders ranged less than 1, indicating a decreasing effect of the studied parameters on the moment and shear responses of internal sections. However, the factors were greater than 1 in the case of exterior girders, showing that railing increased the demand on the edge parts of the superstructure.

As shown in Figure 4.3, MF values showed a decreasing trend in moment responses of interior girders when railing height increased; however, the effect was

TABLE 4.4
Model Estimation Results–Slab Bridges

Loading	Section	Effect	Variable[a]	Parameter Estimate	Standard Error	t-Statistic
Single-Lane	Interior Strip	Moment (1)	constant	1.035	0.024	43.7
			$\overline{h_r}$	-1.700	0.082	-20.8
			$\overline{h_r}^2$	0.732	0.073	10.0
			$\overline{tg\theta}$	-0.456	0.037	-12.3
			$\overline{h_r tg\theta}$	0.430	0.061	7.0
		Shear (2)	constant	0.758	0.072	10.6
			$\overline{h_r}$	-0.820	0.095	-8.7
	Exterior Strip	Moment (3)	constant	0.079	0.014	5.5
			$\overline{h_r}$	1.658	0.056	29.8
			$\overline{h_r}^2$	-0.690	0.050	-13.8
			$\overline{tg\theta}$	-0.136	0.024	-5.7
			$\overline{h_r tg\theta}$	-0.138	0.040	-3.4
		Shear (4)	constant	0.057	0.034	1.7
			$\overline{h_r}$	1.341	0.116	11.6
			$\overline{h_r}^2$	-0.422	0.104	-4.0
			$\overline{tg\theta}$	0.312	0.052	5.9
			$\overline{h_r tg\theta}$	-0.361	0.087	-4.2
Multiple-Lane	Interior Strip	Moment (5)	constant	1.038	0.023	44.3
			$\overline{h_r}$	-1.352	0.081	-16.8
			$\overline{tg\theta}$	0.521	0.073	7.2
			$\overline{h_r tg\theta}$	-0.737	0.037	-20.2
		Shear (6)	constant	0.988	0.056	17.5
			$\overline{h_r}$	-0.459	0.075	-6.2
			$\overline{tg\theta}$	-0.362	0.072	-5.0
	Exterior Strip	Moment (7)	constant	0.107	0.015	7.1
			$\overline{h_r}$	1.635	0.058	28.1
			$\overline{h_r}^2$	-0.697	0.053	-13.3
			$tg\theta$	-0.168	0.025	-6.7
			$\overline{h_r tg\theta}$	-0.240	0.042	-5.7
		Shear (8)	constant	0.130	0.042	3.1
			$\overline{h_r}$	0.913	0.070	13.1
			$\overline{tg\theta}$	0.267	0.072	3.7
			$\overline{h_r tg\theta}$	-0.339	0.119	-2.8

[a] Transformed variables.

TABLE 4.5
Proposed Modification Factor Formulations–Slab Bridges

Loading	Section	Effect	MF[a] Formulation		*RSS*	R^2
Single-Lane	Interior Strip	Moment	$1-0.02h_r+0.0002h_r^2-0.3tg\theta+0.006h_r tg\theta$	(1)	0.04	0.98
		Shear	$1-0.004h_r$	(2)	0.85	0.72
	Exterior Strip	Moment[b]	$1.2+0.2h_r-0.002h_r^2-1.1tg\theta^{1.5}-0.02h_r tg\theta$	(3)	0.02	0.99
		Shear	$1.4+0.07h_r+1.4tg\theta-0.03h_r tg\theta$	(4)	0.08	0.96
Multiple-Lane	Interior Strip	Moment	$1-0.01h_r-0.5tg\theta+0.008h_r tg\theta$	(5)	0.12	0.94
		Shear	$1-0.003h_r-0.2tg\theta$	(6)	0.53	0.68
	Exterior Strip	Moment[b]	$1.2+0.2h_r-0.002h_r^2-1.4tg\theta^{1.5}-0.04h_r tg\theta$	(7)	0.02	0.99
		Shear	$1.6+0.09h_r+1.6tg\theta-0.04h_r tg\theta$	(8)	0.16	0.92

Note:
h_r = railing height (in.), w_d = diaphragm width (in.), θ = skew angle (deg.).
[a] MF is 1 for all cases when h_r and θ are equal to 0.
[b] Range of application $0^\circ \le \theta \le 45^\circ$.

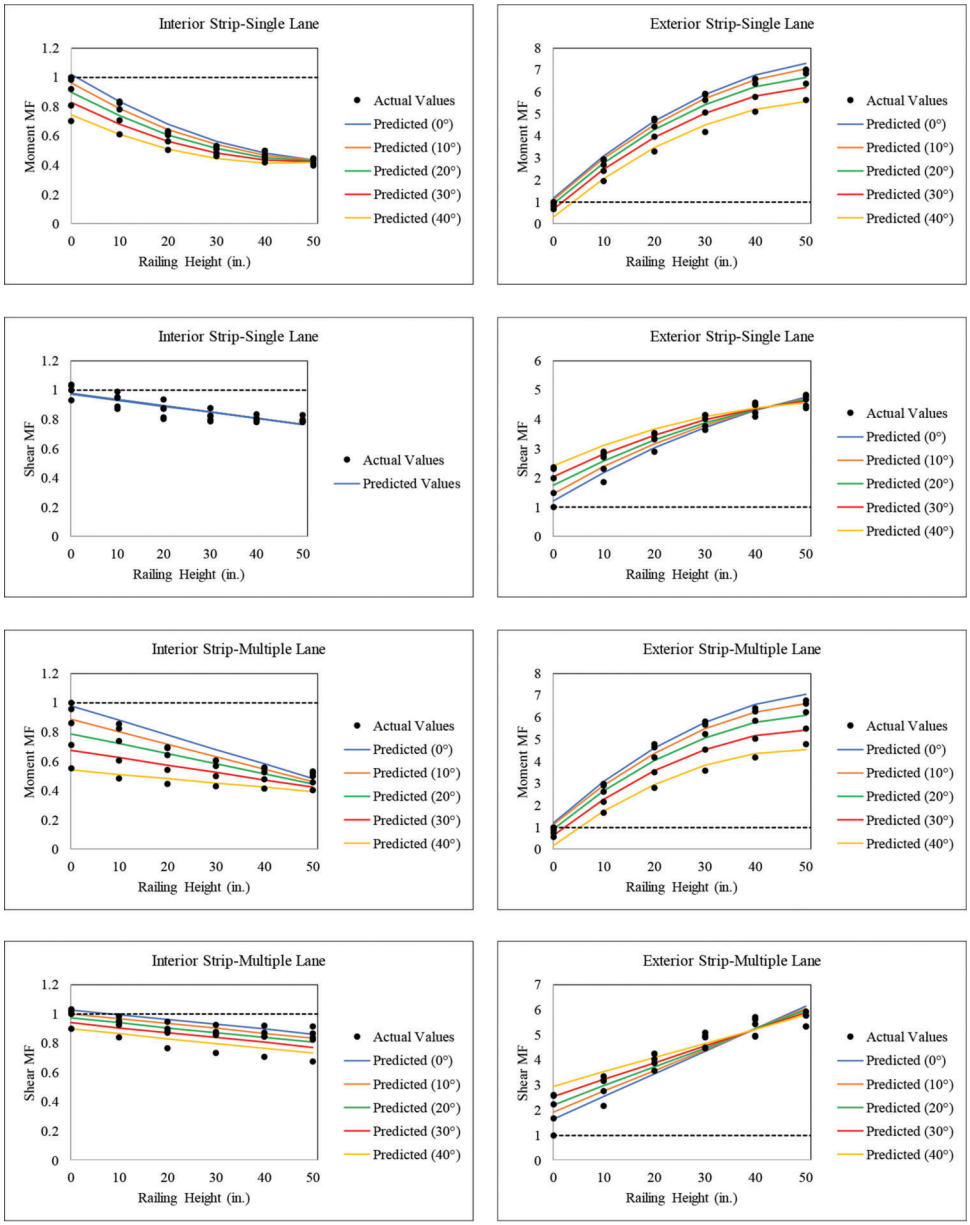

Figure 4.2 Proposed modification factors compared to actual data (FE analysis)–slab.

negligible on shear results. The opposite trend was observed in exterior girder results. As reported in Table 4.7, MF formulations specified a decreasing trend with an increase in diaphragm width in demand for interior girders. This effect was negligible in exterior beams. In general, the effect of railing and diaphragm parameters was described using linear trendlines in regression models. The impact of skew parameter on moment and shear responses was expressed by tangential forms with different power values.

4.6 Proposed Modification Factor Verification

Regression models are mainly used to define a proper mathematical function that relates the dependent variable to independent ones. When a regression function is finalized based on available data, its reliability to predict the future (unobserved) data should be examined. In this study, the effect of variables was studied on reference bridges (slab and T-beam), and modification factors were proposed using regression models. Therefore, the performance of the MF formulations was assessed for bridges with geometrical features (span length, deck width, slab thickness, girder dimensions, etc.) different from those of reference slab and T-beam bridges. This verification indicated how well the regression model could predict the effect of studied parameters in bridges not included in the regression procedure.

The results of proposed MF formulations were compared to those obtained from available skew modification

TABLE 4.6
Model Estimation Results–T-Beam Bridges

Loading	Section	Effect	Variable[a]	Parameter Estimate	Standard Error	t-Statistic
Single-Lane	Interior Girder	Moment (9)	constant	0.954	0.015	65.5
			$\overline{h_r}$	-0.533	0.016	-32.4
			$\overline{tg\theta^{1.5}}$	-0.339	0.016	-21.2
			$\overline{w_d}$	-0.185	0.016	-11.3
		Shear (10)	constant	0.892	0.038	23.2
			$\overline{w_d}$	-1.400	0.189	-7.4
			$\overline{w_d}^2$	0.972	0.177	5.5
			$\overline{w_d tg\theta}$	-0.326	0.085	-3.8
	Exterior Girder	Moment (11)	constant	0.379	0.012	30.7
			$\overline{h_r}$	0.697	0.014	50.1
			$\overline{tg\theta^{1.5}}$	-0.267	0.014	-19.7
			$\overline{w_d}$	-0.073	0.014	-5.3
		Shear (12)	constant	0.095	0.026	3.7
			$\overline{h_r}$	0.653	0.041	15.9
			$\overline{tg\theta}$	0.830	0.043	19.2
			$\overline{h_r tg\theta}$	-0.658	0.069	-9.5
Multiple-Lane	Interior Girder	Moment (13)	constant	0.936	0.016	58.6
			$\overline{h_r}$	-0.200	0.018	-11.1
			$\overline{tg\theta^{1.5}}$	-0.658	0.018	-36.8
			$\overline{w_d}$	-0.171	0.018	-9.3
		Shear (14)	constant	1.029	0.012	85.6
			$\overline{tg\theta}$	-0.646	0.028	-23.1
			$\overline{w_d tg\theta}$	-0.365	0.036	-10.2
	Exterior Girder	Moment (15)	constant	0.354	0.009	38.7
			$\overline{h_r}$	0.620	0.013	48.8
			$\overline{tg\theta^{1.5}}$	-0.326	0.013	-25.8
		Shear (16)	constant	0.175	0.032	5.4
			$\overline{h_r}$	0.777	0.052	15.0
			$\overline{tg\theta}$	0.171	0.058	2.9
			$\overline{h_r tg\theta}$	-0.781	0.090	-8.7

Note:
[a]Transformed variables.

TABLE 4.7
Proposed Modification Factors–T-Beam Bridges

Loading	Section	Effect	MF[a] Formulation		*RSS*	R^2
Single-Lane	Interior Girder	Moment	$1-0.004h_r-0.114tg\theta^{1.5}-0.004w_d$	(9)	0.14	0.96
		Shear	$1-0.03w_d+0.001{w_d}^2-0.006w_d tg\theta$	(10)	1.49	0.72
	Exterior Girder	Moment	$1+0.007h_r-0.125tg\theta^{1.5}-0.002w_d$	(11)	0.10	0.98
		Shear	$1+0.003h_r+0.166tg\theta-0.003h_r tg\theta$	(12)	0.35	0.91
Multiple-Lane	Interior Girder	Moment	$1-0.001h_r-0.193tg\theta^{1.5}-0.003w_d$	(13)	0.17	0.96
		Shear	$1-0.227tg\theta-0.009w_d tg\theta$	(14)	0.22	0.97
	Exterior Girder	Moment	$1+0.008h_r-0.181tg\theta^{1.5}$	(15)	0.08	0.98
		Shear	$1+0.004h_r+0.04tg\theta-0.004h_r tg\theta$	(16)	0.54	0.83

Note:
h_r = railing height (in.), w_d = diaphragm width (in.), è = skew angle (deg.).
[a]MF is 1 for all cases when h_r, w_d, and θ are equal to 0.

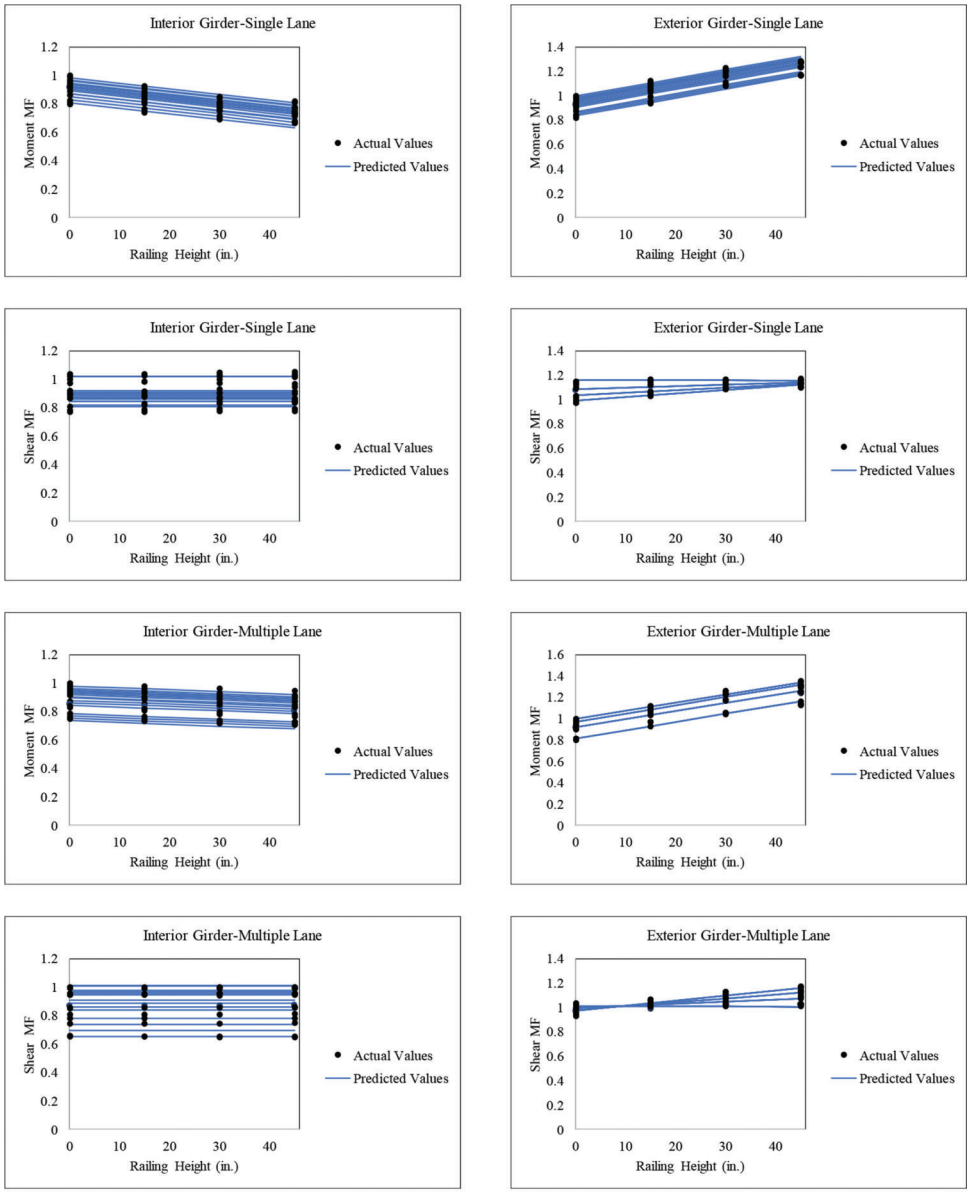

Figure 4.3 Proposed modification factors compared to actual data (FE analysis)–T-beam.

factors in the LRFD specifications for slab and T-beam bridges. In this comparison, the value of 0 was considered for the edge-element parameters ($h_r = w_d = 0$ *in.*) in proposed MF formulations consistent with LRFD assumptions.

4.6.1 Comparison of Proposed and LRFD Skew Modification Factors

In this research's parametric study, skewed superstructures combined with secondary elements were modeled to investigate the possible interaction between these parameters and assess the reliability of available skew correction factors. In the AASHTO LRFD specifications, correction factors are specified to adjust moment/shear demand in skewed bridges as expressed in Equation 3.1 to Equation 3.3.

In slab bridges, the AASHTO formulation is specified for moment responses in the interior section of slab bridges for all loading configurations. This factor was compared with the proposed MF for moment response in interior strips when $h_r = 0$ *in*, (see Table 4.8). As shown in Figure 4.4, the proposed formula could capture the decreasing trend specified in the LRFD skew factor when the skew angle increased. However, code-specified provisions seemed slightly conservative compared to corresponding FE results. The discrepancy between the results increased for larger skew values by up to 11% and 31% for the skew of 40 degree in single and multiple-lane loading, respectively.

In T-beam bridges, moment (in all girders) and shear (in exterior girder) responses should be adjusted in skewed girder bridges using skew modification factor provisions in AASHTO specifications. The skew factors

TABLE 4.8
LRFD and Proposed Skew Modification Factors Comparison

Bridge	Effect	Girder	LRFD Skew MF	Proposed Skew MF	
				Single-Lane	Multiple-Lane
Slab	Moment	Interior	$1.05-0.25tg\theta$	$1.02-0.33tg\theta$	$1.02-0.53tg\theta$
T-Beam	Moment	Interior	$1-0.128tg\theta^{1.5}$	$1-0.114tg\theta^{1.5}$	$1-0.193tg\theta^{1.5}$
		Exterior		$1-0.125tg\theta^{1.5}$	$1-0.181tg\theta^{1.5}$
	Shear	Exterior	$1+0.169tg\theta$	$1+0.166tg\theta$	$1+0.042tg\theta$

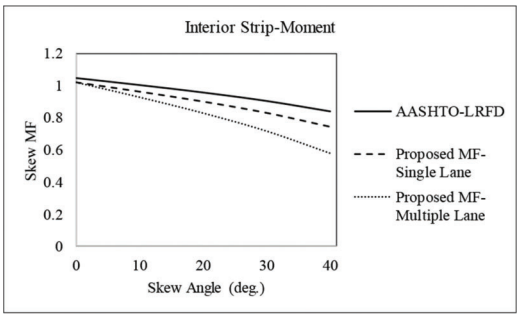

Figure 4.4 LRFD and proposed skew factor comparison in slab bridges.

are a function of bridge length, deck thickness, girder spacing/dimensions, and skew angle. The formulations are identical for single and multiple-lane loading configurations. The geometrical dimensions of average T-beam bridge were replaced in AASHTO skew factor formulations and were compared to corresponding ones obtained from regression models with $h_r = d_w = 0$ *in*, as reported in Table 4.8.

As shown in Figure 4.5, the proposed formulations could capture decreasing and increasing trends expressed in LRFD skew factors for moment and shear demands, respectively, when the skew angle increased. The results obtained from the two approaches matched perfectly for single-lane loading applications with a difference of less than 1% on average. However, current formulation values seemed slightly conservative compared to FE results for multiple-lane loading cases with a difference of less than 9% on average.

In both bridge types, the skew factor formulations approximated using the regression method shared a similar mathematical form to the code-specified provisions with slightly different coefficients in multiple-lane loading cases. Considering that the LRFD formulations were developed using a comprehensive study on a large sample of girder (365) and slab (130) actual bridges, the consistency between the results verified the reliability of the method adopted in this study for railing and end-diaphragm MF propositions.

Due to consistency observed between the FE analysis results and AASHTO recommendations for skew correction, modifications were not proposed for this parameter, and MF formulations were finalized for railing and diaphragm effects as reported in Table 4.9. It should be noted that according to discussion presented in Section 3.5.4, the *interior MFs* obtained from Table 4.9 should be increased by factor of 1.1 (shear) and 1.2 (moment) for cases of continuous slab bridges (see Figure 3.19). Also, proposed MFs for T-beam bridges are only applicable to single-span cases since edge-effect was found to be negligible for these cases (refer to Section 3.5.4).

4.6.2 Verification of Proposed MFs in Random Bridges

To evaluate the performance of the proposed MF formulations, sample bridges were randomly selected from the Indiana bridges dataset. In this process, box-plots were used as a standard tool to visualize the data variability for each geometrical parameter. The main characteristics of a box-plot are shown in Figure 4.6. Box-plots were graphed for slab and T-beam datasets, for parameters such as span length, deck width, slab thickness, skew angle, and girder spacing/dimension shown in Figure 4.7 and Figure 4.8, respectively. These graphs displayed the distribution of data and indicated outlier cases. Using these plots, selected bridges with characteristics within the outlier range (shown with dots in the graphs) were disregarded and replaced with another bridge.

A total of twenty single-span slab and T-beam bridge samples (ten of each type) were randomly selected and modeled in 3D. Sample bridge characteristics are summarized in Table 4.11 (T-beam) and Table 4.10 (slab). The distribution of the selected bridge samples within each category is represented in Figure 4.7 and Figure 4.8 (e.g., S1 represents Sample 1). Each bridge superstructure was firstly modeled and analyzed as a non-skewed bridge without edge-elements. Then, secondary components were added to the model, moment, and shear responses were obtained, and demand ratios (MFs) were calculated using Equation 4.1.

In 3D modeling of slab sample superstructures, representative cross-section dimensions of edge-elements found in Indiana bridges were considered with a height of 12 in. and 33 in. representing standard curb and E706-BRSF railing, respectively. For T-beam cases, a railing height of 24 in. consistent with E706-BRPP configuration was included in bridge 3D models. Skew angle and diaphragm width values are reported in Table 4.11 and Table 4.10 for each bridge sample.

MFs obtained from FE analysis were compared to those calculated using the proposed formulations for each bridge sample. Figure 4.9 and Figure 4.10

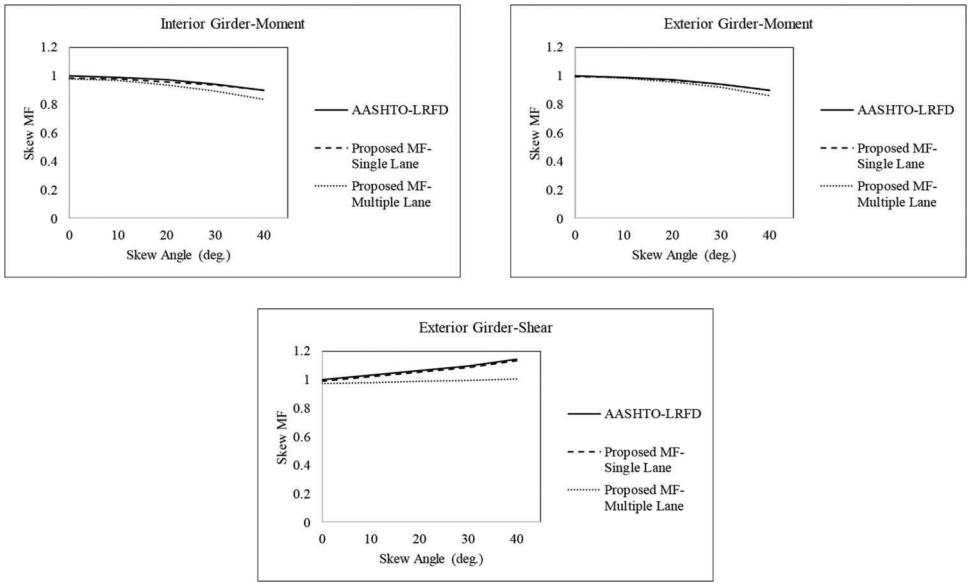

Figure 4.5 LRFD and proposed skew modification factors comparison in T-beam bridges.

TABLE 4.9
Proposed Railing and Diaphragm Modification Factors (Single-Span Bridges)

Bridge	Loading	Section	Effect	Railing MF	Diaphragm MF
Slab	Single-Lane	Interior Strip	Moment	$1-h_r(0.02+0.006tg\theta)+0.0002h_r^2$	–
			Shear	$1-0.004h_r$	
		Exterior Strip	Moment	$1.2+h_r(0.2-0.02tg\theta)-0.002h_r^2$	
			Shear	$1.4+h_r(0.07-0.03tg\theta)$	
	Multiple-Lane	Interior Strip	Moment	$1-h_r(0.01+0.008tg\theta)$	
			Shear	$1-0.003h_r$	
		Exterior Strip	Moment	$1.2+h_r(0.2-0.04tg\theta)-0.002h_r^2$	
			Shear	$1.6+h_r(0.09-0.04tg\theta)$	
T-Beam	Single-Lane	Interior Girder	Moment	$1-0.004h_r$	$1-0.004w_d$
			Shear	–	$1-w_d(0.03-0.006tg\theta)+0.001w_d^2$
		Exterior Girder	Moment	$1+0.007h_r$	$1-0.002w_d$
			Shear	$1+h_r(0.003-0.003tg\theta)$	–
	Multiple-Lane	Interior Girder	Moment	$1-0.001h_r$	$1-0.003w_d$
			Shear	–	$1-0.009w_dtg\theta$
		Exterior Girder	Moment	$1+0.008h_r$	–
			Shear	$1+h_r(0.004-0.004tg\theta)$	–

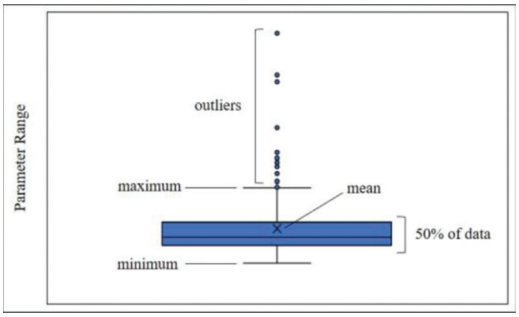

Figure 4.6 Box-plot characteristics.

illustrate a comparison between the results obtained from the two approaches for slab and T-beam samples, respectively. In the graphs, modification factors obtained using proposed formulations and FE analysis are represented as "predicted" and "actual" MF, respectively, and black dashed line represents the 1:1 line. Moreover, Root Mean Square Error (RMSE), as a measure of the differences between predicted and observed value were calculated and is reported in the graphs for each case.

A comparison of the results is shown in Figure 4.9 and Figure 4.10 and indicated that regression models could predict MFs in samples that were not included in the original modeling process. Results obtained from MF formulations (prediction) and 3D models (actual) were scattered closely around the 1:1 line. The discrepancy between the results was inevitable, considering that samples considered for the verification process

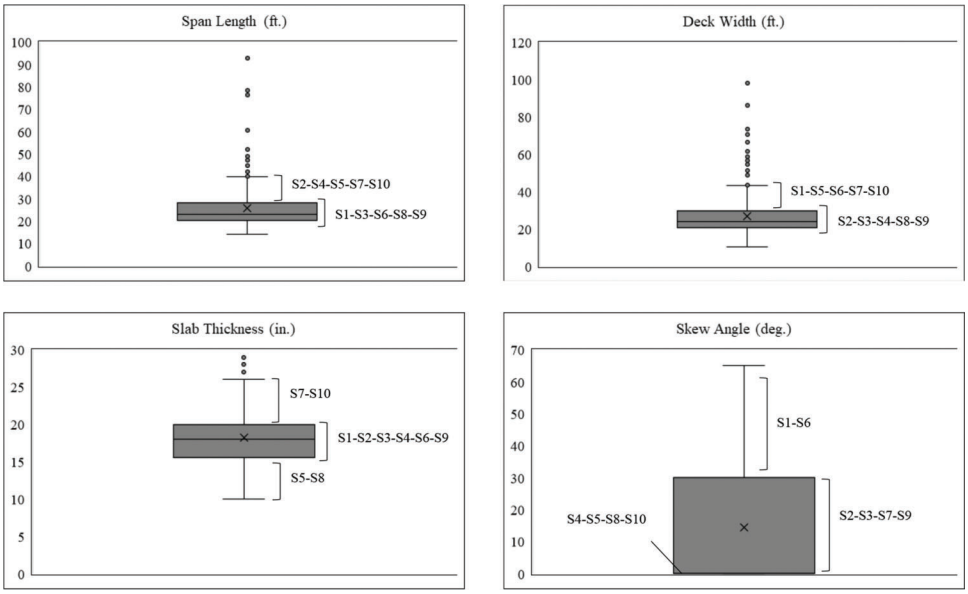

Figure 4.7 Box-plots for slab samples.

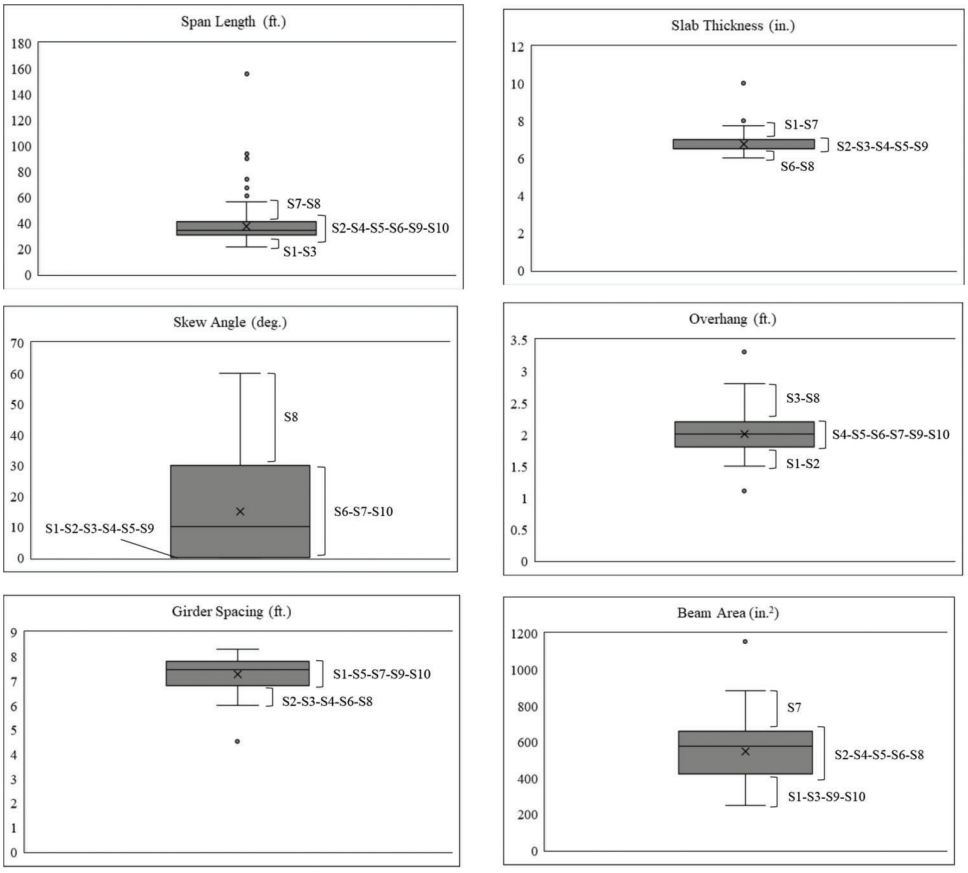

Figure 4.8 Box-plots for T-beam samples.

TABLE 4.10
T-Beam Bridge Samples Information

Sample No.	Span Length (ft.)	Deck Width (ft.)	Slab Thickness (in.)	Girder Width/ Height (in.)	Girder Spacing (in.)	Overhang Length (ft.)	Skew Angle (deg.)	Diaphragm Width (in.)
1	28.0	34.0	7.25	19.0 / 20.0	92.4	1.6	0°	15
2	36.0	29.4	6.50	16.5 / 26.0	78.0	1.7	0°	18
3	24.0	38.3	6.50	16.5 / 18.0	80.4	2.4	0°	15
4	36.0	28.8	6.50	16.5 / 35.0	75.6	1.8	0°	12
5	40.0	33.4	6.50	24.0 / 25.5	87.6	2.1	0°	12
6	36.5	29.2	6.25	16.5 / 25.5	75.6	2.0	10°	10
7	45.0	32.2	7.50	22.0 / 33.0	81.6	2.0	15°	18
8	44.0	43.0	6.00	24.0 / 24.0	75.0	2.8	35°	18
9	30.0	42.6	6.50	16.5 / 20.5	93.6	1.8	0°	12
10	32.0	31.4	6.50	16.5 / 24.0	82.8	1.9	25°	0

TABLE 4.11
Slab Bridge Samples Information

Sample No.	Span Length (ft.)	Deck Width (ft.)	Slab Thickness (in.)	Skew Angle (deg.)
1	27.5	32.4	15.5	44°
2	33.0	23.9	18.0	15°
3	28.2	30.0	18.0	30°
4	35.6	25.6	19.0	0°
5	21.4	26.5	13.0	0°
6	26.0	32.0	18.0	45°
7	37.2	36.0	25.0	25°
8	21.8	24.5	15.0	0°
9	25.9	24.0	18.0	5°
10	38.7	31.8	25.0	0°

were different in geometrical features than those of reference bridges used in the regression procedure.

In slab samples, the average RMSE of 0.07 was obtained for predictions of interior strip modification factors. This value was 0.42 for those of exterior strips. Since root mean square error shares the same unit as data under investigation, a range of data should be considered when interpreting the size of this error. In this case, RMSE values could be considered relatively small, bearing in mind that range of MF values for interior strips between 0 to 1 and for exterior strips between 1 to 6. In T-beam samples, the average RMSE of 0.07 is relatively small, considering the variation range of 0 to 1.4 for MFs in interior and exterior girders.

To compare the size of the errors for different cases in slab and T-beam samples with different range of data, RMSEs were normalized according to the range of data in each category. To do so, Normalized Root Mean Square Error (NRMSE) values were calculated by dividing RMSEs by the average of actual data in each data set. NRMSEs reported in Figure 4.9 and Figure 4.10 ranged between 7%–13% and 4%–10% in slab and T-beam samples, respectively indicating that all MF models resulted in comparable levels of prediction of performance.

4.7 Summary of Findings

Regression analysis was performed to fit the observed data into mathematical formulations. Results of regression analysis were provided in forms of modification factors as a function of edge-element dimensions, i.e., railing height and diaphragm width. The modification factor formulations were proposed for moment and shear demand in interior and exterior sections in a bridge superstructure. Residuals, adjusted R-squared, and t-ratio statistics were used to evaluate the performance of regression models. A good agreement was observed between the predicted (regression) and observed (3D models) values with adjusted R-squared of 89.8% and 91.4% on average for slab and T-beam models, respectively. The average residuals were 0.228 in slab and 0.386 in T-beam bridges.

The prediction power of proposed MF formulations was assessed for twenty randomly selected bridges with geometrical properties different from those of reference slab and T-beam bridges. This verification indicated how well the regression model could predict the effect of studied parameters in bridges not included in the regression procedure. The superstructure of selected bridge samples was modeled in 3D (including

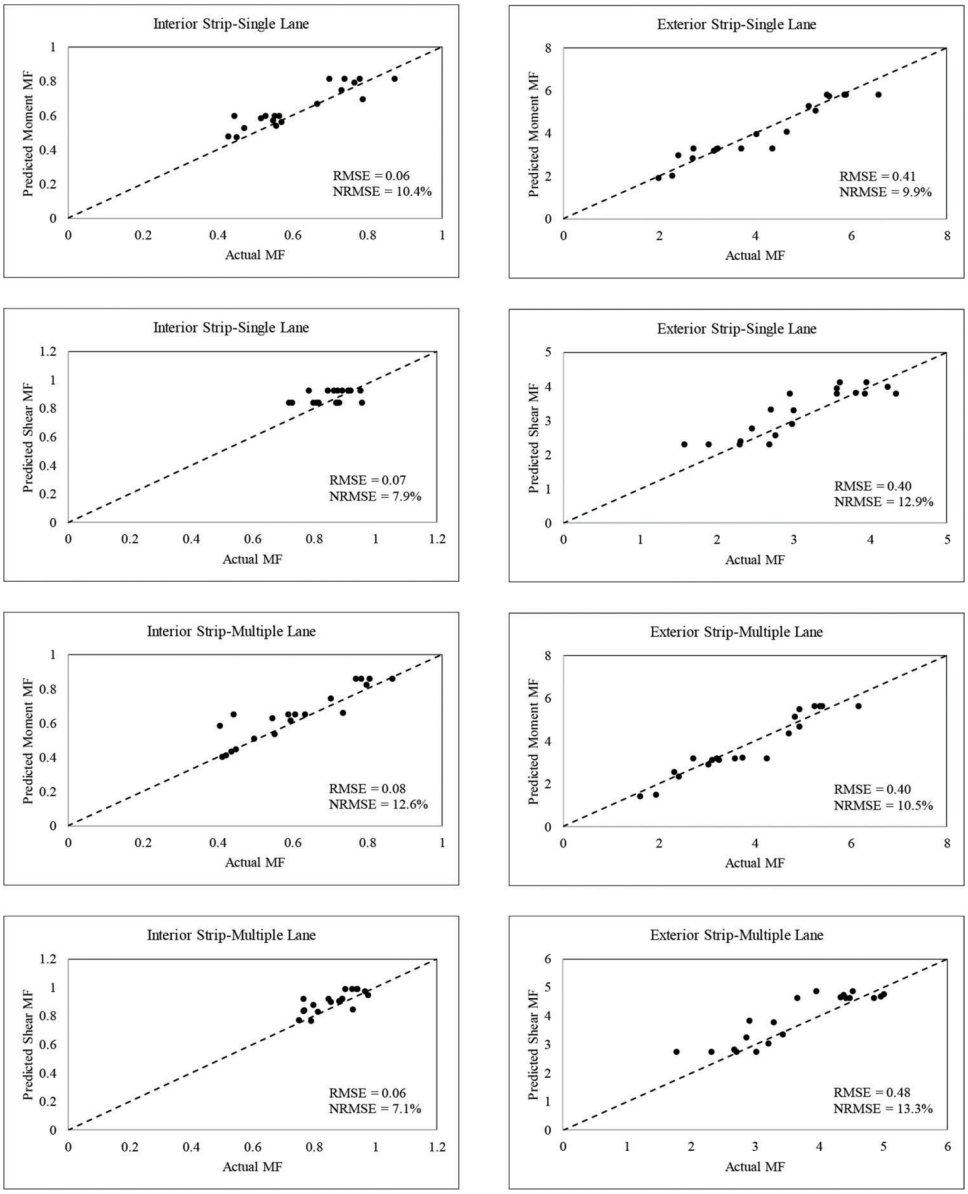

Figure 4.9 Comparison of predicted and actual (from FE analysis) MFs–slab samples.

non-structural components), and live load demand was estimated. An acceptable discrepancy was observed between the results obtained from MF formulations (prediction) and 3D models (actual) with normalized root mean square error of 10% and 7% on average in slab and T-beam samples, respectively.

Moreover, the results of proposed skew MF formulations were compared to those in the LRFD specifications for slab and T-beam bridges. The results obtained from the two approaches agreed well for single-lane loading cases, however, LRFD results were slightly conservative in multiple-lane loading cases. Therefore, modifications were not proposed for skew parameter, and MF formulations were finalized for railing and diaphragm effects. Moreover, the consistency observed in this comparison verified the reliability of the method adopted in this study for railing and end-diaphragm MF propositions.

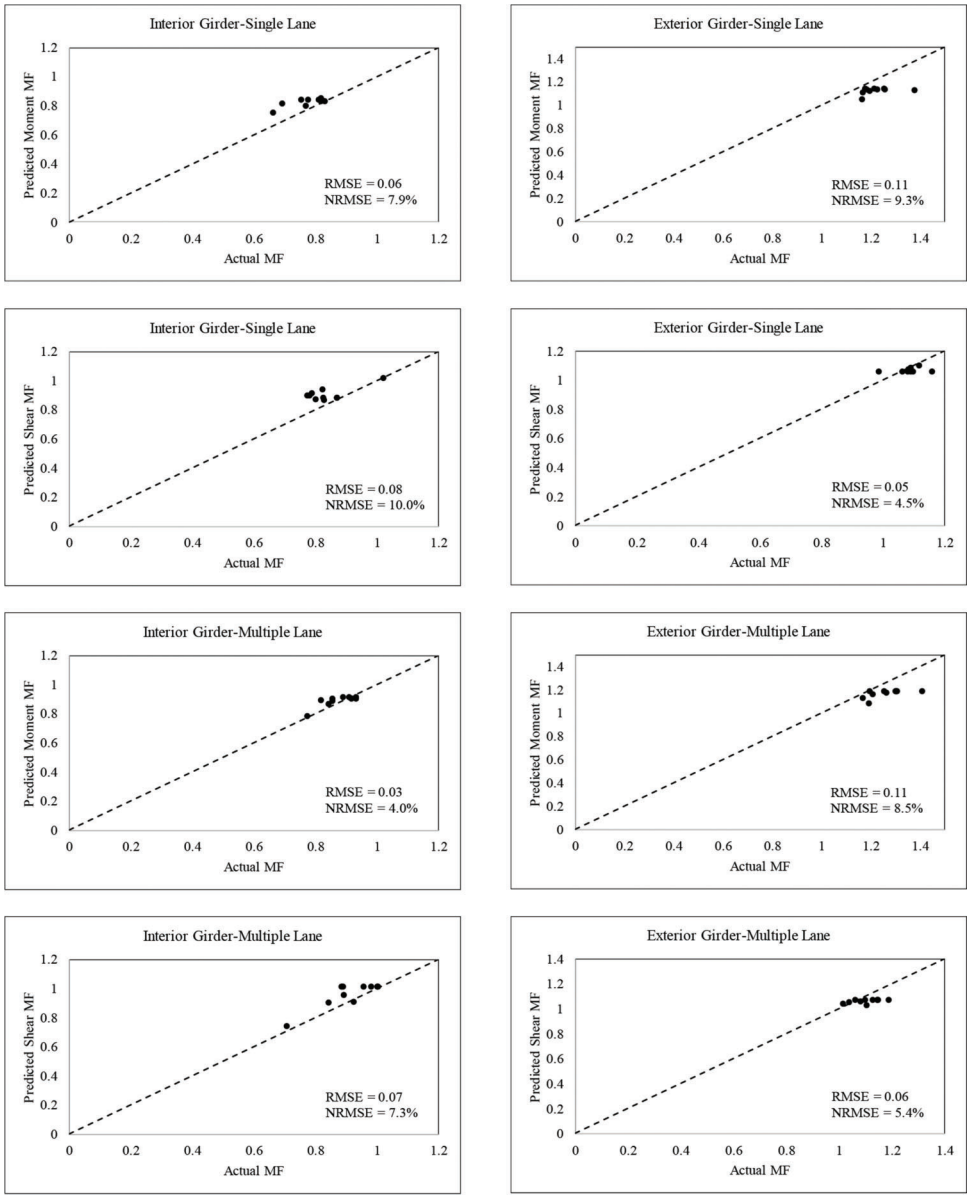

Figure 4.10 Comparison of predicted and actual (from FE analysis) MFs–T-beam samples.

5. SUMMARY OF FINDINGS, CONCLUSIONS, DELIVERABLES, IMPLEMENTATION, AND EXPECTED BENEFITS

5.1 Summary of Findings

This project focused on the investigating an improved methodology for the live load estimation in slab and T-beam reinforced concrete bridges in Indiana using the tools of 3D analysis. To this end, four tasks were conducted, and the findings of each task are summarized below.

Task 1. Identification of Key Parameters

A focused review of available literature on the live load distribution factor formulation was conducted to identify gaps and limitations in current demand estimate provisions in LRFD specifications. Moreover, the National Bridge Inventory (NBI) database for the state of Indiana was surveyed to establish the statistical distribution of bridge parameters and determine the typical bridge configurations to be considered in this project. Common ranges of geometrical characteristics such as number of spans, maximum span length, number of traffic lanes, curb-to-curb width, and deck skew angle were compiled using the data in the NBI. A hypothetical reference bridge was defined with average geometrical properties observed in the NBI dataset and review of bridge drawings.

Task 2. Analysis Program

A parametric study was conducted to assess the impact of geometrical parameters, including railing height, skew angle, and diaphragm width on moment and shear demand

in slab and T-beam bridges. Using finite element analysis, parameters were varied one at a time in the reference bridge model, and live load responses were obtained for both shear and moment. Railing height was confirmed as a parameter that produced the most drastic change in moment and shear demands in bridges with respect to the reference models. When railing height was increased, moment and shear demands increased in exterior sections of both bridge types. This resulted in a demand reduction in interior parts. The same effect was observed with the addition of diaphragms in single-span T-beam bridges, resulting in reduced moment and shear responses in interior girders.

Task 3. Statistical Analysis

Statistical analysis was performed to assess the impact of edge-stiffening on demand in slab and T-beam bridges. Shear and moment responses obtained from 3D models with different variables were compared to those of the reference model. Regression analysis was performed to define a proper mathematical function that relates the effect of secondary elements to demand estimates in different parts of the bridge superstructure. Statistical tests such as analysis of residuals, the goodness of fit, and t-statistics were performed to evaluate the performance of regression models. Regression models could capture the decreasing/increasing trend observed in actual data obtained from the FE analysis with high overall fit and low residuals for both bridge types.

Task 4. Identification and Verification of Proposed Modification Factors

The regression results were proposed in forms of modification factors to existing AASHTO formulations. The proposed modification factors are a function of edge-element dimensions, i.e., railing height and diaphragm width. The modification factor formulations were proposed for moment and shear demand in interior and exterior sections in a bridge superstructure. The reliability of modification factors to predict the unobserved data was examined on a sample of slab and T-beam bridges (ten each) randomly selected from the Indiana bridge dataset. Acceptable agreement was observed between the results obtained from regression and 3D models. Moreover, a comparison between skew factors obtained from regression analysis and corresponding LRFD skew provisions showed adequate consistency between the results. This finding served as verification for the method used in this research to propose railing and diaphragm modifications factors.

5.2 Conclusions and Recommendations

Based on the study results, the following conclusions and recommendations are presented for consideration and possible implementation.

- A parametric study associated with demand estimation showed a substantial effect of geometric features on the distribution of loads over the bridge width. The study showed that railing height, deck skew, and diaphragm width in T-beam bridges had a substantial impact on moment and shear values.
- Effects from the presence of edge components on demand of interior sections are not reflected in the methodology outlined in AASHTO specifications and may be a source of overestimation or underestimation of bridges response. Modifications to current live load distribution factor formulations have been identified to better represent the moment and shear responses observed from 3D finite element analysis.
- Potential improvements of current procedures have been proposed based on statistical studies that compared live load demand obtained from FE analysis to corresponding 2D results. The proposed modification factors address the limitations of the current procedure. The objective of modifying DFs was based on the expectation that INDOT could continue to use 2D analysis in the rating bridges and overload vehicle permits.
- The modification factors proposed in this study are intended to better represent the favorable effects of non-structural elements on demand calculations for interior parts of superstructures. Moreover, they improve the accuracy of demand estimates in exterior sections by providing formulation as a function of edge component's geometry i.e., railing height.
- The presence of railing has a substantial influence on stress distribution in the bridge superstructure, causing higher stress concentrations in exterior strips and reducing stresses in interior ones. The application of proposed railing factors to current DF formulations could reflect this effect on demand evaluation. This formulation applies to any edge components such as railing, parapet, and curb properly anchored to the deck.
- The diaphragms were found to reduce moment and shear responses in interior girders. Their effect was found to be negligible on the response of exterior girders. Applying the proposed diaphragm factors incorporates the beneficial effect of end-diaphragms in demand estimates of T-beam bridges.
- The study showed results for the effect of skew on moment and shear forces were consistent with LRFD skew correction factors, and therefore, no modification is proposed for this parameter. However, in some cases, the skew parameter is presented in railing/diaphragm modification factor formulations to reflect the joint effect observed between the parameters.
- Proposed modification factors were obtained for single-span bridges. In the case of continuous T-beam bridges, edge-effect was found to be negligible. In the case of slab bridges, the factors should be used in multiple-span bridges considering discussion presented in Section 3.5.4 and Section 4.6.1 on decreased edge-stiffening efficacy for continuous bridges. It is also necessary to exercise caution when applying the factors to bridges with geometries greatly different from the average bridges used in this study.
- Findings of this study suggest that the addition of edge components such as curbs, railings, and sidewalk could be considered as a potential rehabilitation technique for bridges that exhibit border-line load rating results in the interior sections of the bridge superstructure provided that the non-structural elements are properly designed, reinforced, and anchored to the deck. Caution should be exercised in these members' construction practices since they attract a great amount of stress. The presence of

TABLE 5.1
Proposed LRFD Live Load Modification Factors for Slab and T-Beam Single-Span Bridges

Bridge	Loading	Section	Effect	Railing MF[a]	Diaphragm MF[a]
Slab	Single-Lane	Interior Strip	Moment	$1-h_r(0.02+0.006tg\theta)+0.0002h_r^2$	NA
			Shear	$1-0.004h_r$	
		Exterior Strip	Moment	$1.2+h_r(0.2-0.02tg\theta)-0.002h_r^2$	
			Shear	$1.4+h_r(0.07-0.03tg\theta)$	
	Multiple-Lane	Interior Strip	Moment	$1-h_r(0.01+0.008tg\theta)$	
			Shear	$1-0.003h_r$	
		Exterior Strip	Moment	$1.2+h_r(0.2-0.04tg\theta)-0.002h_r^2$	
			Shear	$1.6+h_r(0.09-0.04tg\theta)$	
T-Beam	Single-Lane	Interior Girder	Moment	$1-0.004h_r$	$1-0.004w_d$
			Shear	NA	$1-w_d(0.03-0.006tg\theta)+0.001{w_d}^2$
		Exterior Girder	Moment	$1+0.007h_r$	$1-0.002w_d$
			Shear	$1+h_r(0.003-0.003tg\theta)$	NA
	Multiple-Lane	Interior Girder	Moment	$1-0.001h_r$	$1-0.003w_d$
			Shear	NA	$1-0.009w_d tg\theta$
		Exterior Girder	Moment	$1+0.008h_r$	NA
			Shear	$1+h_r(0.004-0.004tg\theta)$	NA

Note:
h_r =railing height (in.), w_d = diaphragm width (in.), θ = skew angle (deg.)
[a]MF is 1 for all cases when h_r, w_d, and θ are equal to 0.

joints or improper reinforcement detailing might create cracking due to stress concentrations.

5.3 Deliverables, Implementation, and Expected Benefits

In response to discussions with the Study Advisor Committee, the proposed modifications to the AASHTO LRFD live load distribution factors would be implemented as shown in Table 5.1. The values in Table 5.1 would be applied to the shear and bending moments from the 2D conventional load rating procedure using current distribution factors. When more than one factor applies, these are to be applied simultaneously to the shear and bending moments from the 2D CLR procedure.

The modifications are given for interior and exterior strips in slab bridges, and exterior and interior beams in T-beam bridges for cases of single and multi-lane loading configurations. The modification factors are in terms of the height of the concrete railing, and width of concrete diaphragm. In the cases identified in Section 5.2 where a parameter was shown not to influence the demand, the term NA (Not Applicable) is shown in the table.

Updated DFs can be used in conventional load rating methods to incorporate 3D effects while maintaining the simplicity of load rating procedures. The findings of this study may be used to update the demand evaluation process in the BrR platform used by the Indiana Department of Transportation for rating and design practices as discussed in the final section of this report. This proposed modification would benefit a great population of Indiana bridges that might be conservatively identified as structurally deficient or functionally obsolete. In particular, those bridges that show no signs of structural deficiency and, with proper maintenance, could be expected to serve well into the future.

REFERENCES

AASHTO. (2014). *LRFD bridge design specifications* (7th ed.). American Association of State Highway and Transportation Officials.

AASHTO. (2002). *Standard specifications for highway bridges* (17th ed.). American Association of State Highway and Transportation Officials.

Amer, A., Arockiasamy, M., & Shahawy, M. (1999). Load distribution of existing solid slab bridges based on field tests. *Journal of Bridge Engineering*, *4*(3), 189–193. https://doi.org/10.1061/(ASCE)1084-0702(1999)4:3(189)

Azizinamini, A., Boothby, T. E., Shekar, Y., & Barnhill, G. (1994a, November). Old concrete slab bridges. I: Experimental investigation. *Journal of Structural Engineering*, *120*(11), 3284–3304. https://doi.org/10.1061/(ASCE)0733-9445(1994)120:11(3284)

Azizinamini, A., Shekar, Y., Boothby, T. E., & Barnhill, G. (1994b, November). Old concrete slab bridges. II: Analysis. *Journal of Structural Engineering*, *120*(11), 3305–3319. https://doi.org/10.1061/(asce)0733-9445(1994)120:11(3305)

Bakht, B., & Moses, F. (1988). Lateral distribution factor for highway bridges. *Journal of Structural Engineering*, *114*(8), 1785–1803. https://doi.org/10.1061/(ASCE)0733-9445(1988)114:8(1785)

Barr, P. J., Eberhard, M. O., & Stanton, J. F. (2001). Live-load distribution factors in prestressed concrete girder bridges. *Journal of Bridge Engineering*, *6*(5), 298–306. https://doi.org/10.1061/(ASCE)1084-0702(2001)6:5(298)

Bell, E. S., Lefebvre, P. J., Sanayei, M., Brenner, B., Sipple, J. D., & Peddle, J. (2013, October). Objective load rating of a steel-girder bridge using structural modeling and health monitoring. *Journal of Structural Engineering*, *139*(10), 1771–1779. https://doi.org/10.1061/(ASCE)ST.1943-541X.0000599

Bishara, A. G., Chuan Liu, M., & El-Ali, N. D. (1993, February). Wheel load distribution on simply supported skew I-beam composite bridges. *Journal of structural Engi-*

neering, *119*(2), 399–419. https://doi.org/10.1061/(ASCE)0733-9445(1993)119:2(399)

Cai, C. S., & Shahawy, M. (2004). Predicted and measured performance of prestressed concrete bridges. *Journal of Bridge Engineering*, *9*(1), 4–13. https://doi.org/10.1061/(ASCE)1084-0702(2004)9:1(4)

Cai, C. S., Araujo, M., Chandolu, A., Avent, R. R., & Alaywan, W. (2007). Diaphragm effects of prestressed concrete girder bridges: Review and discussion. *Practice Periodical on Structural Design and Construction*, *12*(3), 161–167. https://doi.org/10.1061/(ASCE)1084-0680(2007)12:3(161)

Cai, C. S., Shahawy, M., & Peterman, R. J. (2002). Effect of diaphragms on load distribution of prestressed concrete bridges. *Transportation Research Record*, *1814*, 47–54. https://doi.org/10.3141/1814-06

Chen, Y. (1999). Distribution of vehicular loads on bridge girders by the FEA using ADINA: Modeling, simulation, and comparison. *Journal of Computers & Structures*, *72*(1–3), 127–139. https://doi.org/10.1016/S0045-7949(99)00032-2

Conner, S., & Huo, X. S. (2006, March). Influence of parapets and aspect ratio on live-load distribution. *Journal of Bridge Engineering*, *11*(2), 188–196. https://doi.org/10.1061/(ASCE)1084-0702(2006)11:2(188)

Eamon, C. D., & Nowak, A. S. (2002). Effects of edge-stiffening elements and diaphragms on bridge resistance and load distribution. *Journal of Bridge Engineering*, *7*(5), 258–266.

Eamon, C. D., & Nowak, A. S. (2004). Effects of secondary elements on bridge structural system reliability considering moment capacity. *Journal of Structural Safety*, *26*(1), 29–47. https://doi.org/10.1016/S0167-4730(03)00020-1

Eom, J., & Nowak, A. S. (2001). Live load distribution for steel girder bridges. *Journal of Bridge Engineering*, *6*(6), 489–497. https://doi.org/10.1061/(ASCE)1084-0702(2001)6:6(489)

Everitt, B. S. (2002). *The Cambridge dictionary of statistics* (2nd ed.). Cambridge University Press.

FHWA. (2019). Federal Highway Administration Database. Retrieved from https://www.fhwa.dot.gov/bridge/britab.cfm

Frederick, G. R., & Tarhini, K. M. (2000). Wheel load distribution in concrete slab bridges. *Computing in Civil and Building Engineering*, 1236–1239. https://doi.org/10.1061/40513(279)161

Green, T., Yazdani, N., Spainhour, L., & Cai, C. S. (2002). Intermediate diaphragm and temperature effects on concrete bridge performance (Paper No. 02-3627). *Transportation Research Record*, *1814*, 83–90. https://doi.org/10.3141/1814-10

Hasançebi, O., & Dumlupinar, T. (2013). Detailed load rating analyses of bridge populations using nonlinear finite element models and artificial neural networks. *Journal of Computer and Structures*, *128*, 48–63. https://doi.org/10.1016/j.compstruc.2013.08.001

Hays, C. O., Larry, J., Sessions, M., & Berry, A. J. (1986). Further studies on lateral load distribution using a finite element method. *Transportation Research Record*, *1072*, 6–14.

Huo, X. S., Wasserman, E. P., & Zhu, P. (2004). Simplified method of lateral distribution of live load moment. *Journal of Structural Engineering*, *9*(4), 382–390. https://doi.org/10.1061/(ASCE)1084-0702(2004)9:4(382)

Jáuregui, D. V., & Barr, P. J. (2004, November). Nondestructive evaluation of the I-40 Bridge over the Rio Grande River. *Journal of Performance of Constructed Facilities*, *18*(4), 195–204. https://doi.org/10.1061/(ASCE)0887-3828(2004)18:4(195)

Khaleel, M. A., & Itani, R. Y. (1990, September). Live-load moments for continuous skew bridges. *Journal of Structural Engineering*, *116*(9), 2361–2373. https://doi.org/10.1061/(ASCE)0733-9445(1990)116:9(2361)

Khaloo, A. R., & Mirzabozorg, H. (2003). Load distribution factors in simply supported skew bridges. *Journal of Bridge Engineering*, *8*(4), 241–244.

Kuzmanovic, B. O., & Sanchez, M. R. (1986). Lateral distribution of live loads on highway bridges. *Journal of Structural Engineering*, *112*(8), 1847–1862.

Mabsout, M. E., Tarhini, K. M., Frederick, G. R., & Kobrosly, M. (1997a). Influence of sidewalk and railing on wheel load distribution in steel girder bridges. *Journal of Bridge Engineering*, *2*(3), 88–96.

Mabsout, M. E., Tarhini, K. M., Frederick, G. R., & Tayar, C. (1997b). Finite-element analysis of steel girder highway bridges. *Journal of Bridge Engineering*, *2*(3), 83–87.

Mabsout, M. E., Tarhini, K. M., Frederick, G. R., & Kesserwan, A. (1998, August). Effect of continuity on wheel load distribution in steel girder bridges. *Journal of Bridge Engineering*, *3*(3), 103–110.

Mabsout, M., Tarhini, K., Jabakhanji, R., & Awwad, E. (2004). Wheel load distribution in simply supported concrete slab bridges. *Journal of Bridge Engineering*, *9*(2), 147–155.

Menassa, C., Mabsout, M., Tarhini, K., & Frederick, G. (2007, March). Influence of skew angle on reinforced concrete slab bridges. *Journal of Bridge Engineering*, *12*(2), 205–214. http://dx.doi.org/10.1061/(ASCE)1084-0702(2007)12:2(205)

Sanayei, M., Reiff, A. J., Brenner, B. R., & Imbaro, G. R. (2016, April). Load rating of a fully instrumented bridge: Comparison of LRFR approaches. *Journal of Performance in Construction Facility*, *30*(2), 04015019. https://doi.org/10.1061/(ASCE)CF.1943-5509.0000752

Seok, S., Ravazdezh, F., Haikal, G., & Ramirez, J. A. (2019). *Strength assessment of older continuous slab and T-beam reinforced concrete bridges* (Joint Transportation Research Program Publication No. FHWA/IN/JTRP-2019/13), West Lafayette, IN: Purdue University. https://doi.org/10.5703/1288284316924

Shahawy, M., & Huang, D. (2001, July). Analytical and field investigation of lateral load distribution in concrete slab-on-girder bridges. *ACI Structural Journal*, *98*(4), 590–599.

Spokoiny, V., & Dickhaus, T. (2014). *Basics of modern mathematical statistics*. Springer Publications.

Tarhini, K. M., & Frederick, G. R. (1992). Wheel load distribution in I-girder highway bridges. *Journal of Structural Engineering*, *118*(5), 1285–1294.

Upton, G., & Cook, I. (2014). *A dictionary of statistics* (3rd ed.). Oxford University Press.

Washington, S. P., Karlafits, M. G., & Mannering, F. (2010, December). *Statistical and econometric methods for transportation data analysis* (2nd ed.). Chapman and Hall.

Weisberg, S. (2005). *Applied linear regression* (3rd ed.). Wiley Interscience Publications.

Winters, R., Winters, A., & Amedee, R. G. (2010). Statistics: A brief overview. *The Ochsner Journal*, *10*(3), 213–216.

Yousif, Z., & Hindi, R. (2007). AASHTO-LRFD live load distribution for beam-and-slab bridges: Limitations and applicability. *Journal of Bridge Engineering*, *12*(6), 765–773. https://doi.org/10.1061/(ASCE)1084-0702(2007)12:6(765)

Zokaie, T., Osterkamp, T. A., & Imbsen, R. A. (1991, March). *Distribution of wheel loads on highway bridges* (NCHRP 12-26/1 Final Report). National Cooperative Highway Research Program. http://onlinepubs.trb.org/onlinepubs/nchrp/docs/NCHRP12-26_FR.pdf

About the Joint Transportation Research Program (JTRP)

On March 11, 1937, the Indiana Legislature passed an act which authorized the Indiana State Highway Commission to cooperate with and assist Purdue University in developing the best methods of improving and maintaining the highways of the state and the respective counties thereof. That collaborative effort was called the Joint Highway Research Project (JHRP). In 1997 the collaborative venture was renamed as the Joint Transportation Research Program (JTRP) to reflect the state and national efforts to integrate the management and operation of various transportation modes.

The first studies of JHRP were concerned with Test Road No. 1—evaluation of the weathering characteristics of stabilized materials. After World War II, the JHRP program grew substantially and was regularly producing technical reports. Over 1,600 technical reports are now available, published as part of the JHRP and subsequently JTRP collaborative venture between Purdue University and what is now the Indiana Department of Transportation.

Free online access to all reports is provided through a unique collaboration between JTRP and Purdue Libraries. These are available at http://docs.lib.purdue.edu/jtrp.

Further information about JTRP and its current research program is available at http://www.purdue.edu/jtrp.

About This Report

An open access version of this publication is available online. See the URL in the citation below.

Ravazdezh, F., Ramirez, J. A., & Haikal, G. (2021). *Improved live load distribution factors for use in load rating of older slab and T-beam reinforced concrete bridges* (Joint Transportation Research Program Publication No. FHWA/IN/JTRP-2021/06). West Lafayette, IN: Purdue University. https://doi.org/10.5703/1288284317303